Stem and soil nitrous oxide fluxes from rainforest and cacao agroforest on highly weathered soils in the Congo Basin

Najeeb A. Iddris[1], Marife D. Corre[1], Martin Yemefack[2,3], Oliver van Straaten[1,4], Edzo Veldkamp[1]

[1]Soil Science of Tropical and Subtropical Ecosystems, University of Goettingen, Goettingen, 37077, Germany

[2] International Institute of Tropical Agriculture, Yaoundé, Cameroon

[3] Now at: Sustainable Tropical Solutions (STS), Yaoundé, Cameroon

[4] Now at: Northwest German Forest Research Institute, Goettingen, 37079, Germany

Correspondence to: N. A. Iddris (niddris@gwdg.de)

Abstract. Although tree stems act as conduits for greenhouse gases (GHG) produced in the soil, the magnitudes of tree contributions to total (soil + stem) nitrous oxide (N_2O) emissions from tropical rainforests on heavily weathered soils remain unknown. Moreover, soil GHG fluxes are largely understudied in African rainforests, and the effects of land-use change on these gases are identified as an important research gap in the global GHG budget. In this study, we quantified the changes in stem and soil N_2O fluxes with forest conversion to cacao agroforestry. Stem and soil N_2O fluxes were measured monthly for a year (2017–2018) in four replicate plots per land use at three sites across central and southern Cameroon. Tree stems consistently emitted N_2O throughout the measurement period, and were positively correlated with soil N_2O fluxes. ^{15}N-isotope tracing from soil mineral N to stem-emitted $^{15}N_2O$ as well as correlations between temporal patterns of stem N_2O emissions, soil-air N_2O concentration, soil N_2O emissions, and vapor pressure deficit suggest that N_2O emitted by the stems originated predominantly from N_2O produced in the soil. Forest conversion to extensively managed, mature (> 20 years old) cacao agroforestry had no effect on stem and soil N_2O fluxes. The annual total N_2O emissions were 1.55 ± 0.20 kg N ha^{-1} yr^{-1} from the forest and 1.15 ± 0.10 kg N ha^{-1} yr^{-1} from cacao agroforestry, with tree N_2O emissions contributing 11 to 38% for forests and 8 to 15% for cacao agroforestry. These substantial contributions of tree stems to total N_2O emissions highlight the importance of including tree-mediated fluxes in ecosystem GHG budgets. Taking into account that our study sites' biophysical characteristics represented two-thirds of the humid rainforests in the Congo Basin, we estimated a total N_2O source strength for this region of 0.18 ± 0.05 Tg N_2O yr^{-1}.

1. Introduction

The trace gas nitrous oxide (N_2O) has become the main stratospheric ozone depleting substance produced by human activities (Ravishankara et al., 2009), and is after carbon dioxide and methane (CH_4) the most important anthropogenic greenhouse gas (GHG) (Denman et al., 2007). Humid

tropical soils are considered one of the most important global N_2O sources (Denman et al., 2007; Werner et al., 2007a), with tropical rainforests alone estimated to contribute between 0.9 to 4.5 Tg N_2O-N yr^{-1} to the global N_2O source of about 16 Tg N_2O-N yr^{-1} (Bouwman et al., 1995; Breuer et al., 2000; Werner et al., 2007a). However, ground-based, bottom-up N_2O emission estimates appear to be in stark contrast to the high emissions estimated from top-down approaches such as modelling and global N_2O atmospheric inversions (Huang et al., 2008; Thompson et al., 2014). Nevertheless, there exists considerable uncertainty in both approaches (Davidson and Kanter, 2014), especially for the tropics (Valentini et al., 2014). Recent studies suggest two possible reasons for large uncertainties in bottom-up approaches: "missing" emission pathways such as trees (Welch et al., 2019), and a strong geographic bias of measured N_2O fluxes from tropical forests.

Most of the studies on soil N_2O fluxes from tropical ecosystems were conducted in South and Central America (Davidson and Verchot, 2000; Matson et al., 2017; Neill et al., 2005; Wolf et al., 2011), tropical Asia (Hassler et al., 2017; Purbopuspito et al., 2006; Veldkamp et al., 2008; Verchot et al., 2006; Werner et al., 2006) and Australia (Breuer et al., 2000; Kiese et al., 2003). Africa remains the continent with the least published field studies on soil N_2O fluxes from the tropical forest biome. After the pioneering work by Serca et al. (1994), very few field studies have been conducted, most of which were either not replicated with independent plots or only with short measurement campaigns (Castaldi et al., 2013; Gütlein et al., 2018; Wanyama et al., 2018; Werner et al., 2007b). The remaining studies were based on laboratory incubations, which cannot be translated to actual field conditions. Consequently, field–based studies with sufficient spatial and temporal coverage are critical for improving the highly uncertain N_2O sink and source estimates for Africa (Kim et al., 2016b; Valentini et al., 2014).

The Congo Basin is the second largest intact tropical forest in the world and constitutes one of the most important carbon (C) and biodiversity reservoirs globally. Behind the DR Congo,

Cameroon is the second highest deforested country in the Congo Basin with about 75% of its forest being subject to pressure from other land uses including agroforestry (Dkamela, 2010). Conversion of forests to traditional cacao agroforestry (CAF) systems have well been documented in Cameroon (Saj et al., 2013; Sonwa et al., 2007; Zapfack et al., 2002). Presently, an estimated 400,000 hectares is under CAF on small family farms of approximately one to three hectares (Kotto et al., 2002; Saj et al., 2013). These CAF systems are commonly established under the shade of the forests' remnant trees, and are characterised by absence of fertilizer inputs and low yields of up to 1 t cacao beans ha^{-1} (Saj et al., 2013).

Changes in land use have been found to affect soil N_2O emissions due to changes in soil N availability, vegetation and management practices such as N fertilization (Corre et al., 2006; Davidson and Verchot, 2000; Groffman et al., 2000; Hassler et al., 2017; Veldkamp et al., 2020). In particular, unfertilized agroforestry and agricultural systems have been found to have comparable N_2O fluxes as those from the reference forests (Hassler et al., 2017), whereas N-fertilized systems tend to have higher N_2O fluxes than the previous forest due to elevated soil mineral N following fertilization (Verchot et al., 2006). This is in line with postulations of the conceptual hole-in-the-pipe (HIP) model, which suggest that the magnitude of N_2O emissions from the soil are largely controlled first by soil N availability and second by soil water content (Davidson et al., 2000). A systematic comparison between a reference land use and a converted system for quantifying land-use change effects on GHG fluxes is virtually lacking for the Congo Basin, and thus an important knowledge gap in the GHG budget of Africa (Valentini et al., 2014).

Tree stems have been found to act as conduits for soil N_2O in wetlands, mangroves and well-drained forests (Kreuzwieser et al., 2003; Rusch and Rennenberg, 1998; Welch et al., 2019), facilitating the transport from the soil, where N_2O are produced or consumed by microbial nitrification and denitrification processes, to the atmosphere. Findings of strong declines in N_2O emissions with increasing stem height (Barba et al., 2019; Díaz-Pinés et al., 2016; Rusch and

Rennenberg, 1998; Wen et al., 2017) suggest that N_2O is mainly emitted through the stems and less likely through the leaves. Trees adapted to wetlands and mangroves have aerenchyma systems through which N_2O can be transported from the soil into the tree by both gas diffusion and transpiration stream, with exchange to the atmosphere predominantly through the stem lenticels (Rusch and Rennenberg, 1998; Wen et al., 2017). However, for trees on well-drained soils, a different transport mechanism appears to be dominant: transpiration drives the xylem sap flow in which dissolved N_2O is transported from the soil to the tree and emitted to the atmosphere through the stem surface and stomata (Machacova et al., 2013; Wen et al., 2017). Recent evidence shows that trees can also act as N_2O sinks (Barba et al., 2019; Machacova et al., 2017), highlighting the need for further research of the stem N_2O flux magnitudes and their mechanisms.

The most important soil parameters found to influence tree-stem N_2O fluxes include soil water content (Machacova et al., 2016; Rusch and Rennenberg, 1998), soil N_2O fluxes (Díaz-Pinés et al., 2016; Wen et al., 2017), soil temperature (Machacova et al., 2013) and soil-air N_2O concentration within the rooting zone (Machacova et al., 2013; Wen et al., 2017). These studies also reported environmental parameters, such as air temperature and vapour pressure deficit, to drive stem N_2O fluxes due to their influence on transpiration (O'Brien et al., 2004). For temperate forests on a well-drained soil, annual stem N_2O fluxes have been found to contribute up to 10% of the ecosystem N_2O emissions (Wen et al., 2017). However, until now, there is no ground-based spatial extrapolation of the contribution of stem N_2O emissions from tropical forests on well-drained soils. Hence, there is a need for concurrent quantifications of the contributions of stem and soil N_2O fluxes so as to provide insights on the source strengths of N_2O emissions from tropical African land uses and to improve estimates of N_2O emissions from the region.

Our present study addresses these knowledge gaps by providing year-round measurements of stem and soil N_2O fluxes from forests and converted CAF systems with spatially replicated plots in the Congo Basin as well as stem N_2O fluxes of 23 tree species that have not

been measured before. Our findings contribute to the much-needed improvement of GHG budget from this region. Our study aimed to (i) assess whether trees in tropical rainforests and CAF are important conduits of N_2O, (ii) quantify changes in soil-atmosphere N_2O fluxes with forest conversion to CAF, and (iii) determine the temporal and spatial controls of stem and soil N_2O fluxes. We hypothesized that (i) stem and soil N_2O fluxes from these extensively managed CAF systems (unfertilized and manual harvest) will be comparable to the natural forests, and (ii) the seasonal pattern of stem emissions will parallel that of soil N_2O emissions and both will have similar soil and climatic controlling factors.

2. Materials and methods

2.1 Study area and experimental design

Our study was conducted at three study sites located in southern and central Cameroon, where natural forests are predominantly converted to CAF (Sonwa et al., 2007). Sites in the southern region were located around the villages of Aloum (2.813° N, 10.719° E; 651 m above sea level, asl) and Biba Yezoum (3.158° N, 12.292° E; 674 m asl), and the third site was located around the village of Tomba (3.931° N, 12.430° E; 752 m asl) in the central region (Fig. B1). The mean annual air temperature across the three sites is 23.5 °C (Climate-Data.org, 2019), and the soil temperature ranged from 21.6–24.4 °C during our measurement period from May 2017 to April 2018. The study sites span an annual precipitation from 1576 mm yr^{-1} in the central to 2064 mm yr^{-1} in the south of Cameroon (Table A1; Climate-Data.org, 2019). Precipitation occurs in a bimodal pattern, with two dry seasons (< 120 mm monthly rainfall) occurring from July to August and December to February. All sites are situated on heavily weathered soils classified as Ferralsols (FAO classification; IUSS Working Group WRB, 2015). Geologically, Tomba and Biba Yezoum are underlain by middle to superior Precambrian basement rocks (metamorphic schists, phyllites and quartzites), whereas Aloum site is situated on inferior Precambrian basement rocks (inferior gneiss and undifferentiated gneiss) (Gwanfogbe et al., 1983).

At each of the three sites, we studied two land–use systems: the reference forest and the converted CAF system. Additional information on vegetation and site characteristics are reported in Table A1. These CAF sites were established right after clearing the natural forests, where remnant forest trees were retained by farmers to provide shade for understorey cacao trees (*Theobroma cacao*). Cacao planting and localised weeding were all done manually using hand tools. Interviews of farm owners indicated that there had been no mineral fertilization in any of the CAF sites. The ages of the CAF since conversion varied between 22 and ~ 45 years.

We selected four replicate plots (50 m x 50 m each with a minimum distance of 100 m between plots) per land-use type within each site (Fig. B1), totalling to 24 plots that were all located on relatively flat topography. Within each plot, all stems including cacao trees with a diameter at breast height (DBH) ≥ 10 cm were identified and measured for DBH and height. We conducted N_2O flux measurements, soil and meteorological parameters in the inner 40 m × 40 m area within each plot to minimize edge effects. To check that soil conditions were comparable between the reference forests and converted CAF, we compared a land-use-independent soil characteristic, i.e. clay content at 30–50 cm depth, between these land uses at each site. Since we did not find significant differences in clay contents between the forest and CAF at each site (Table 1), we inferred that land-use types within each site had comparable initial soil characteristics prior to conversion and any differences in N_2O fluxes and soil controlling factors can be attributed to land-use conversion.

For measurements of stem N_2O fluxes, we selected six cacao trees per replicate plot in the CAF, and six trees representing the most dominant species within each replicate plot in the forest, based on their importance value index (IVI) (Table A2). The species IVI is a summation of the relative density, relative frequency and relative dominance of the tree species (Curtis and McIntosh, 1951). For a given species, the relative density refers to its total number of individuals in the four forest plots at each site; the relative frequency refers to its occurrence among the four

forest plots; and the relative dominance refers to its total basal area in the four forest plots, all expressed as percentages of all species. These 24 trees measured at each site (6 trees x 4 forest plots) included nine species in Aloum site, seven species in Biba Yezoum site, and 10 species in Tomba site (species are specified in Fig. 1; Table A2). The trees were measured for stem N_2O fluxes at 1.3 m height above the ground at monthly interval from May 2017 to April 2018. Furthermore, we assessed the influence of tree height on stem N_2O fluxes by conducting additional measurements on 16 individual trees per land use in May 2018; these trees were included in the monthly measurements but were additionally measured at three stem heights (1.3 m, 2.6 m and 3.9 m from the ground) per tree in the forest, and at two heights (1.3 m and 2.6 m) per tree in the CAF due to the limited height of the cacao trees.

For soil N_2O flux measurements, we installed four permanent chamber bases per replicate plot which were randomly distributed within the inner 40 m × 40 m area. We conducted monthly measurements of soil N_2O fluxes from May 2017 to April 2018 as well as meteorological and soil variables known to control N_2O emission (see below).

2.2 Measurement of stem and soil N_2O fluxes

We measured in situ stem N_2O fluxes using stem chambers made from transparent polyethylene-terephthalate foil, as described by Wen et al. (2017). One month prior to measurement, we applied acetic acid-free silicone sealant strips (Otto Seal ® S110, Hermann Otto GmbH, Fridolfing, Germany) of about 1 cm wide at 20 cm apart around the surface of the tree stems (between 1.2 m and 1.4 m heights from the ground) that stayed permanently to ensure that all the stem chambers had air-tight seals (Fig. B2). As many of the measured trees have buttresses (rendering stem chambers impossible to attach at low stem height, e.g. Fig. B2), we chose the measurements at an average of 1.3 m height (or between 1.2–1.4 m), congruent to the standard measurement of DBH. Since chamber installation is quick, chambers were newly installed on each sampling date, using the silicone sealant strips as a mark to ensure that the same

185 0.2 m length stem section was measured. We wrapped a piece of foil (cut approximately 50 cm
186 longer than the measured stem circumference and fitted with a Luer lock sampling port) around
187 each stem. Using a gas-powered heat gun, we "shrank" the top and bottom part of the foil to fit
188 closely onto the silicone strips, leaving 0.2 m length between the top and bottom silicone strips,
189 which served as the chamber for collecting gas samples (Fig. B2). We then wrapped strips of
190 polyethylene foam around the edges of the foil and adjusted the foam tightly using lashing straps
191 equipped with ratchet tensioners (two straps at the top and two at the bottom). The lashing straps
192 adjusted the flexible foam and the foil (on top of the silicone strips) to any irregularities on the
193 bark and ensured an airtight fitting. After installation, we completely evacuated the air inside the
194 stem chamber using a syringe fitted with a Luer lock one-way check valve. Afterwards, we used
195 a manual hand pump to refill the stem chamber with a known volume of ambient outside air for
196 correct calculation of stem N_2O flux. A 25 mL air sample was taken with syringe through the
197 Luer lock sampling port immediately after refilling the stem chamber with ambient air, and then
198 again after 20, 40 and 60 min. Each air sample was immediately stored in pre-evacuated 12 mL
199 Labco exetainers with rubber septa (Labco Limited, Lampeter, UK), maintaining an overpressure.
200 In May 2018, we conducted a ^{15}N tracing experiment at the Tomba site as a follow–on
201 study to elucidate the source of stem N_2O emissions. The tracing was conducted in three replicate
202 plots per land use, where one tree was selected in each plot. Around each selected tree, 290 mg
203 ^{15}N (in the form of $(^{15}NH_4)_2SO_4$ with 98% ^{15}N) dissolved in 8 L distilled water was applied evenly
204 onto the soil surface of 0.8 m^2 around the tree using a watering can (equivalent to 10 mm of rain).
205 The water-filled pore space (WFPS) in the top 5 cm depth was 49 ± 1% and 52 ± 2% for the
206 forest and CAF, respectively, which were within the range of monthly average WFPS of these
207 plots (Fig. 2i). Based on the monthly average soil mineral N concentrations in these plots, the
208 applied ^{15}N was only 20% of the extant mineral N in the top 10 cm soil (resulting to a starting
209 enrichment of 17% ^{15}N), such that we only minimally changed the substrate which could

influence N_2O flux, similar to that described by Corre et al. (2014). Stem and soil $^{15}N_2O$ fluxes were measured one day, seven days and 14 days following ^{15}N application, and on each sampling day gas samples were taken at 0, 30, and 60 min after chamber closure. The gas samples were stored in new pre-evacuated glass containers (100 mL) with rubber septa and transported to the University of Goettingen, Germany for analysis. We also stored $^{15}N_2O$ standards in similar 100 mL glass containers, which were brought to Cameroon and back to Germany, to have the same storage duration as the gas samples in order to check for leakage; we found no difference in $^{15}N_2O$ with the original standard at our laboratory.

We measured soil N_2O fluxes using vented, static chambers made from polyvinyl chloride that were permanently inserted ~ 0.02 m into the soil at least one month prior to the start of measurements, as described in our earlier studies (e.g., Corre et al., 2014; Koehler et al., 2009; Müller et al., 2015). On each sampling day, we covered the chamber bases with vented, static polyethylene hoods (0.04 m^2 in area and ~ 11 L total volume) equipped with Luer lock sampling ports. Soil N_2O fluxes were then determined by taking four gas samples (25 mL each) at 2, 12, 22 and 32 min after chamber closure. The samples were taken with a syringe and immediately injected into pre-evacuated 12 mL exetainers as described above.

Concurrent to the stem and soil N_2O flux measurements, we sampled soil-air N_2O concentrations at 50 cm depth from permanently installed stainless steel probes (1 mm internal diameter) located at ~ 1 m from the measured trees. The stainless steel probes were installed one month prior to the start of measurements. Luer locks were attached to the probes, and on each sampling day the probes were first cleared of any previous accumulation of N_2O concentration by removing 5 mL air volume using a syringe and discarding it. We then took 25 mL gas samples and stored them in pre-evacuated 12 mL exetainers as described above.

2.3 N_2O analysis and flux rate calculation

The N_2O concentrations in the gas samples were analysed using a gas chromatograph equipped with an electron capture detector, a make-up gas of 5% CO_2 – 95% N_2 (SRI 8610C, SRI Instruments Europe GmbH, Bad Honnef, Germany), and an autosampler (AS-210, SRI Instruments). $^{15}N_2O$ was analysed on an isotope ratio mass spectrometer (IRMS) (Finnigan Deltaplus XP, Thermo Electron Corporation, Bremen, Germany). We calculated N_2O fluxes from the linear change in concentrations over time of chamber closure, and adjusted the fluxes with air temperature and atmospheric pressure, measured at each replicate plot on each sampling day. We included zero and negative fluxes in our data analysis.

We up-scaled the measured stem N_2O fluxes (considering trees ≥ 10 cm DBH) to annual values on a ground area in the following steps: (1) the relationship between stem N_2O fluxes and stem heights was modelled from the 16 individual trees per land use (see above) that were measured at multiple heights, from which we observed decreases in stem N_2O fluxes with increasing stem heights. A linear function was statistically the best fit characterizing these decreases in stem N_2O fluxes with height. (2) Using this linear function and considering the stem surface area as a frustum with 20 cm increment, the tree-level N_2O fluxes on each sampling day was calculated for the regularly measured six trees per plot. (3) The annual tree-level N_2O fluxes from these regularly measured six trees per plot were calculated using a trapezoidal interpolation between the tree-level N_2O fluxes (step 2) and measurement day intervals from May 2017 to April 2018. (4) The annual tree-level N_2O fluxes were then extrapolated on a ground–area basis for each replicate plot as follows (Eq. 1):

$$Annual\ stem\ N_2O\ flux\ (kg\ N_2O\text{–}N\ ha^{-1}\ yr^{-1}) = \frac{\left\{\sum\left[\left(\frac{X_{1-24}/DBH_{1-24}}{24}\right)*DBH_n\right]\right\}}{A} \quad (1)$$

where $X_{1\text{-}24}$ and $DBH_{1\text{-}24}$ are the corresponding annual tree-level N_2O flux (kg N_2O-N yr^{-1} of each tree; step 3) and DBH (cm) of each of the 24 measured trees (6 trees x 4 plots) per land use

257 at each site, DBH_n is the individual tree DBH (cm) measured for all trees (with ≥ 10 cm DBH)
258 present within the inner 40 m × 40 m area of each plot (Table A1), Σ is the sum of the annual
259 N_2O fluxes of all trees within each plot (kg N_2O-N yr^{-1}) and A is the plot area (0.16 ha).

260 For step 4 of the CAF plots, the annual stem N_2O flux was the sum of the cacao and shade
261 trees (Table A1); as these shade trees were remnants of the original forest, we used the average
262 annual tree-level N_2O flux of the measured trees in the corresponding paired forest plots
263 multiplied by the actual DBH of the shade trees in the CAF plots. This spatial extrapolation based
264 on trees' DBH of each plot was also supported by the fact that there were no significant
265 differences in stem N_2O fluxes among tree species (Fig. 1).

266 Annual soil N_2O fluxes from each plot were calculated using the trapezoidal rule to
267 interpolate the measured fluxes from May 2017 to Apr. 2018, as employed in our earlier studies
268 (e.g., Koehler et al., 2009; Veldkamp et al., 2013). Finally, the annual N_2O fluxes from each
269 replicate plot were represented by the sum of the stem and soil N_2O fluxes.

270 **2.4 Soil and meteorological variables**

271 We measured soil temperature, WFPS, and extractable mineral N in the top 5 cm depth concurrent
272 to stem and soil N_2O flux measurements on each sampling day. The soil temperature was
273 measured ~1 m away from the soil chambers using a digital thermometer (GTH 175, Greisinger
274 Electronic GmbH, Regenstauf, Germany). We determined soil WFPS and extractable mineral N
275 by pooling soil samples from four sampling locations within 1 m from each soil chamber in each
276 replicate plot. Gravimetric moisture content was determined by oven-drying the soils at 105 °C
277 for 24 h and WFPS was calculated using a particle density of 2.65 g cm^{-3} for mineral soil and our
278 measured soil bulk density (Table 1). Soil mineral N (NO_3^- and NH_4^+) was extracted in the field
279 by putting a subsample of soil into a pre-weighed bottle containing 150 mL 0.5 M K_2SO_4. The
280 bottles were weighed and then shaken for 1 h, and the solution was filtered through pre-washed
281 (with 0.5 M K_2SO_4) filter papers. The extracts were immediately frozen and later transported to

the University of Goettingen, where NH_4^+ and NO_3^- concentrations were analysed using continuous flow injection colorimetry (SEAL Analytical AA3, SEAL Analytical GmbH, Norderstedt, Germany) (described in details by Hassler et al., 2015). The dry mass of soil extracted for mineral N was calculated using the measured gravimetric moisture content.

During each measurement day, we set up a portable weather station in each site to record relative humidity and air temperature over the course of each sampling day at 15 min interval. We calculated vapour pressure deficit (VPD) as the difference between saturation vapour pressure (based on its established equation with air temperature) and actual vapour pressure (using saturation vapour pressure and relative humidity; Allen et al., 1998).

Soil biochemical characteristics were measured in April 2017 at all 24 plots. We collected soil samples from the top 50 cm depth, where changes in soil biochemical characteristics resulting from land-use changes have been shown to occur (van Straaten et al., 2015; Tchiofo Lontsi et al., 2019). In each plot, we collected ten soil samples from the top 0–10 cm, and five soil samples each from 10–30 and 30–50 cm depths; in total, we collected 480 soil samples from the 24 plots. The soil samples were air dried, sieved (2 mm) and transported to the University of Goettingen, where they were dried again at 40 °C before analysis. Soil pH was analysed from 1:4 soil to distilled water ratio. Soil texture for each plot was determined using the pipette method after iron oxide and organic matter removal (Kroetsch and Wang, 2008). Effective cation exchange capacity (ECEC) and exchangeable cation concentrations (Ca, Mg, K, Na, Al, Fe, Mn) were determined by percolating the soil samples with unbuffered 1 M NH_4Cl, and the extracts analysed using inductively coupled plasma-atomic emission spectrometer (ICP-AES; iCAP 6300 Duo VIEW ICP Spectrometer, Thermo Fischer Scientific GmbH, Dreieich, Germany). Soil subsamples were ground and analysed for total organic C and N using a CN analyser (vario EL cube; Elementar Analysis Systems GmbH, Hanau, Germany), and the soil ^{15}N natural abundance signatures were determined using IRMS (Delta Plus; Finnigan MAT, Bremen, Germany). Soil

organic carbon (SOC) and total N stocks were calculated for the top 50 cm in both land uses. We used the bulk density of the reference forest for calculating the SOC and total N stocks of the converted CAF in order to avoid overestimations of element stocks resulting from increases in soil bulk densities following land-use conversion (van Straaten et al., 2015; Veldkamp, 1994).

To evaluate the representativeness of our study area with the rest of the Congo Basin rainforest, we estimated the proportion of the Congo rainforest area which have similar biophysical conditions (elevation, precipitation ranges and soil type) as our study sites (Table A1). Using the FAO's Global Ecological Zone map for the humid tropics, we identified the areal coverage of (*i*) Ferralsols (FAO Harmonized World Soil Database; FAO/IIASA/ISRIC/ISS-CAS/JRC, 2012) with (*ii*) elevation ≤ 1000 m asl (SRTM digital elevation model; Jarvis et al., 2008) and (*iii*) precipitation range between 1,500 and 2,100 mm yr^{-1} (WorldClim dataset; Hijmans et al., 2005) within the six Congo rainforest countries (Fig. B3). This analysis was conducted using QGIS version 3.6.3.

2.5 Statistical analyses

Statistical comparisons between land uses or among sites for stem and soil N_2O fluxes were performed on the monthly measurements and not on the annual values as the latter are trapezoidal interpolations. As the six trees and four chambers per plot were considered subsamples representing each replicate plot, we conducted the statistical analysis using the means of the six trees and of the four chambers on each sampling day for each replicate plot (congruent to our previous studies, e.g., Hassler et al., 2017; Matson et al., 2017). We tested each parameter for normal distribution (Shapiro–Wilk's test) and homogeneity of variance (Levene's test), and applied a logarithmic or square root transformation when these assumptions were not met. For the repeatedly measured parameters, i.e. stem and soil N_2O fluxes and the accompanying soil variables (temperature, WFPS, NH_4^+ and NO_3^- concentrations), differences between land-use types for each site or differences among sites for each land-use type were tested using linear

mixed effect (LME) models with land use or site as fixed effect and replicate plots and sampling days as random effects (Crawley, 2009). We assessed significant differences between land uses or sites using analysis of variance (ANOVA) with Tukey's HSD test.

We also analysed if there were differences in stem N_2O fluxes among tree species across four forest plots at each site as well as across the three sites. Similar LME analysis was carried out with tree species as fixed effect, and the random effects were trees belonging to each species and sampling days; only for this test, we used individual trees as random effect because most of the tree species (selected based on their IVI; see Sect. 2.1.) were not present in all plots, which is typical in species-diverse tropical forest. For soil biochemical characteristics that were measured once (Table1), one-way ANOVA followed by a Tukeys's HSD test was used to assess the differences between land uses or sites for the variables with normal distribution and homogenous variance; if otherwise, we applied Kruskal-Wallis ANOVA with multiple comparison extension test.

To determine the temporal controls of soil and meteorological variables (temperature, WFPS, NH_4^+ and NO_3^- concentrations, soil-air N_2O concentration, VPD) on stem and soil N_2O fluxes, we conducted Spearman's Rank correlation tests using the means of the four replicate plots for each land use on each sampling day. For each land use, the correlation tests were conducted across sites and sampling days (n = 33, from 3 sites × 11 monthly measurements). To determine the spatial controls of soil biochemical characteristics (which were measured once, Table 1) on stem and soil N_2O fluxes, we used the plots' annual N_2O emissions and tested with Spearman's Rank correlation across land uses and sites (n = 24, from 3 sites × 2 land uses × 4 replicate plots). The statistical significance for all the tests were set at $P \leq 0.05$. All statistical analyses were conducted using the open source software R 3.5.2 (R Core Team, 2018).

355 ## 3 Results

356 ### 3.1 Stem N2O emissions

357 Stem N_2O emissions neither differed between forest and CAF at each site (P = 0.15–0.76; Table
358 2) nor among the three sites for each land use (P = 0.16–0.78; Table 2). There were also no
359 differences in stem N_2O emissions among tree species in forest plots at each site as well as across
360 the three sites (P = 0.06–0.39; Fig. 1). For the forests, stem N_2O emissions exhibited seasonal
361 pattern with larger fluxes in the wet season than in the dry season at all sites (all $P < 0.01$; Table
362 A3; Fig. 2a, b, c). However, for the CAF, we observed seasonal differences only at Aloum site
363 ($P < 0.01$; Table A4; Fig. 2a). Contributions of annual stem N_2O emissions reached up to one-
364 third of the total (stem + soil) N_2O emissions from the forests (Table 2).

365 From the ^{15}N-tracing experiment, stem ^{15}N-N_2O emissions mirrored soil ^{15}N-N_2O
366 emissions from both land uses (Fig. 3). One day after ^{15}N addition to the soil, substantial ^{15}N-
367 N_2O were emitted from the stem as well as from the soil. This diminished within two weeks as
368 the added ^{15}N recycled within the soil N cycling processes, diluting the ^{15}N signatures;
369 nevertheless, the ^{15}N signatures of stem- and soil-emitted N_2O remained elevated above the
370 natural abundance level (Fig. 3).

371 Across the study period, stem N_2O emissions from the forests were positively correlated
372 with air temperature, soil-air N_2O concentrations and VPD (Table 3) and negatively correlated
373 with WFPS and $NH4^+$ contents (Table 3). The negative correlation of stem N_2O emissions with
374 WFPS was possibly spurious, as this correlation may have been driven by the autocorrelation
375 between WFPS and air temperature (Spearman's $\rho = -0.59$, $P < 0.01$, $n = 33$). In CAF, stem N_2O
376 emissions were only positively correlated with soil N_2O emissions (Table 3).

377 We detected no difference in WFPS between the forest and CAF (P = 0.15–0.28; Table
378 4) at any of the sites. For the CAF, we detected higher WFPS in the wet season compared to the
379 dry season at two sites ($P < 0.01$; Table A4; Fig. 2g, h) whereas there was no seasonal difference

380 in WFPS for the forests at any sites (P = 0.31–0.92; Table A3; Fig. 2g, h, i). At all the three sites,
381 the dominant form of mineral N was $NH4^+$ (Table 4). There was generally no difference in soil
382 $NH4^+$ and $NO3^-$ between the wet and dry seasons (P = 0.12–0.93), except for the forests at two
383 sites with larger values in the dry than wet season (P < 0.01; Tables S2, S3).

384 **3.2 Soil N_2O emissions**

385 Soil N_2O emissions did not differ between forest and CAF at any site (P = 0.06–0.86; Table 2).
386 Similarly, no differences in soil N_2O emissions were detected among sites for each land use (P =
387 0.26–0.44; Table 2). Soil N_2O emissions exhibited consistent seasonal patterns with larger fluxes
388 in the wet than dry season for both land uses (all P < 0.01; Tables S2, S3; Fig. 2d, e, f).

389 Over the measurement period, soil N_2O emissions from the forests were positively
390 correlated with soil-air N_2O concentrations and negatively correlated with $NH4^+$ contents (Table
391 3). In the CAF, soil N_2O emissions were positively correlated with WFPS and soil-air N_2O
392 concentrations, and negatively correlated with air temperatures (Table 3). We did not detect any
393 correlation between annual total N_2O fluxes and soil physical and biochemical characteristics.
394 This was not surprising as the ranges of these soil characteristics were relatively small among
395 sites, which reduce the likelihood that significant correlations will be detected.

396 **3.3 Soil biochemical characteristics**

397 Soil physical characteristics (clay content, bulk density) did not differ between forest and CAF
398 at any of the sites (Table 1). Across sites, Biba Yezoum had lower clay content compared to the
399 other sites for each land use (P < 0.01). Generally, the forest showed higher SOC and total N
400 compared to the CAF (P < 0.01–0.05; Table 1). Soil ^{15}N natural abundance signatures, as an
401 index of the long-term soil N availability, were generally similar between the forest and CAF
402 except at Aloum site (P < 0.01; Table 1). Soil C/N ratio, another proxy for the long-term soil N
403 status, was higher in the forest than in the CAF at all sites (P < 0.01–0.05). Soil pH and

exchangeable bases were lower in the forest compared to the CAF at all sites and the converse was true for exchangeable Al ($P < 0.01–0.05$; Table 1). Soil ECEC did not differ between the land uses at two sites ($P < 0.01$; Table 1) and all were low congruent to Ferralsol soils.

4 Discussion

4.1 Stem and soil N_2O emissions from the forest

There has been no study on tree stem N_2O emission from Africa, nor has any study been reported for the Congo Basin on soil N_2O emission with year-round measurements and spatial replication. Stems consistently emitted N_2O in both land uses (Table 2; Fig 1, Fig. 2a, b, c), exemplifying that tropical trees on well-drained soils were important contributors of ecosystem N_2O emission. So far, there are only two tree species of tropical lowland forest reported with measurements of stem N_2O emissions (Welch et al., 2019). Our present study included 23 tree species and their comparable stem N_2O emissions, at least from highly weathered Ferralsol soils, across sites over a year of measurements provided support to our spatial extrapolation based on DBH of trees in the sites. Mean stem N_2O fluxes from our study were within the range of those reported for temperate forests (0.01–2.2 μg N m^{-2} stem h^{-1}; Díaz-Pinés et al., 2016; Machacova et al., 2016; Wen et al., 2017), but substantially lower than the reported stem N_2O emissions of 51–759 μg N m^{-2} stem h^{-1} for a humid forest in Panama (Welch et al., 2019). However, Welch et al. (2019) measured stem N_2O emissions at a lower stem height (0.3 m) compared to our study (1.3 m), which may partly explain their much larger N_2O emissions, as other studies reported that larger N_2O emissions occur nearer to the stem base of trees (Barba et al., 2019; Díaz-Pinés et al., 2016). Moreover, the consistently higher stem than soil N_2O emissions found by Welch et al. (2019), which we did not observe in our study, may point to production of N_2O within the stem (e.g., Lenhart et al., 2019). Nonetheless, such high stem N_2O emissions as reported by Welch et al. (2019) have not been observed anywhere else under field conditions. We did not find an effect of tree diameter sizes on stem N_2O fluxes at our study sites. This was due to the narrow range

between the DBH of our measured trees (10–18 cm DBH for cacao trees and 10–30 cm DBH for the forest trees), which reflected the mean stem diameter of trees in our sites (Table A1). Future studies should incorporate trees of wide-ranging diameter size classes, if present at the site, as they may influence N_2O flux estimates at the ecosystem-scale.

Our annual soil N_2O emissions from forests (Table 2) were lower than the reported global average for humid tropical forests (2.81 kg N ha^{-1} yr^{-1}; summarised by Castaldi et al., 2013). In contrast, the N_2O emissions from our forest soils were comparable to those reported for lowland forests on Ferralsol soils in Panama (0.35–1.07 kg N ha^{-1} yr^{-1}; Matson et al., 2017), and lowland forests on Acrisol soils in Indonesia (0.9 and 1.0 kg N ha^{-1} yr^{-1}; Hassler et al., 2017). These were possibly due to the generally similar soil N availability in our forest sites as these forest sites in Panama and Indonesia, indicated by their comparable soil mineral N contents and soil ^{15}N natural abundance signatures.

In comparison with studies from sub-Saharan Africa, annual soil N_2O emissions from our forests were lower than the annual N_2O emissions reported for the Mayombe forest in Congo (2.9 kg N ha^{-1} yr^{-1}; Serca et al., 1994), Kakamega mountain rainforest in Kenya (2.6 kg N ha^{-1} yr^{-1}; Werner et al., 2007b), and Ankasa rainforest in Ghana (2.3 kg N ha^{-1} yr^{-1}; Castaldi et al., 2013), but similar in magnitude as those reported for Mau Afromontane forest in Kenya (1.1 kg N ha^{-1} yr^{-1}; Wanyama et al., 2018). Although these African sites have similar precipitation level and highly weathered acidic soils as our study sites, the Kakamega rainforest in Kenya had higher SOC (7.9–20%) and N contents (0.5–1.6%) in the topsoil layer compared to our forest sites (2.8–4.7% SOC, 0.2–0.4% total N), which may explain its correspondingly higher soil N_2O emissions. The study in Congo (Serca et al., 1994), however, was conducted only in a short campaign (two rainy months and one dry month) with less sampling frequency and spatial replication, which may not be a good representation of the spatial and temporal dynamics of soil N_2O fluxes to achieve annual and large-scale estimate.

4.2 Source of tree stem N_2O emissions and their contribution to total (stem + soil) N_2O emissions

Emitted N_2O from stems were found to originate predominantly from N_2O produced in the soil, as shown by the ^{15}N tracing experiment (Fig. 3). Additionally, the positive correlations of stem N_2O emissions with soil-air N_2O concentrations and soil N_2O emissions (Table 3) suggest that the seasonal variation in stem N_2O emissions (Table A3; Fig. 2) was likely driven by the temporal dynamics of produced N_2O in the soil, which partly supported our second hypothesis. While there has been suggestions of within-tree N_2O production (e.g., Lenhart et al., 2019), our finding from the ^{15}N tracing experiment, combined with the correlations of stem N_2O emissions with VPD and air temperature, pointed to a transport mechanism of dissolved N_2O in soil water by transpiration stream, which has been reported to be important for upland trees that do not have aerenchyma (Machacova et al., 2016; Welch et al., 2019; Wen et al., 2017).

The contributions of up-scaled stem N_2O emissions from our studied forests to total (stem + soil) N_2O emissions (Table 2) were higher than those reported for temperate forests (1–18%; Díaz-Pinés et al., 2016; Machacova et al., 2016; Wen et al., 2017). Given the higher stem N_2O emissions in the wet than dry seasons (Table A3), coupled with the fact that we consistently measured positive fluxes or net stem N_2O emissions throughout our measurement period (Fig. 2), we conclude that tree stems in these well-drained Ferralsol soils were efficient conduits for releasing N_2O from the soil. This has significant implications especially during the rainy season as this pathway bypasses the chance for complete denitrification (N_2O to N_2 reduction) in the soil.

4.3 Factors controlling temporal variability of stem and soil N_2O fluxes

The positive correlation of stem N_2O emissions with VPD and air temperature in the forest suggests for transport of N_2O via sap flow, for which the latter had been shown to be stimulated

with increasing VPD and air temperature (McJannet et al., 2007; O'Brien et al., 2004). Soil water containing dissolved N_2O is transported through the xylem via the transpiration stream and eventually emitted from the stem surface to the atmosphere (Díaz-Pinés et al., 2016; Welch et al., 2019; Wen et al., 2017).

Soil moisture has been shown to affect strongly the seasonal variation of soil N_2O emissions from tropical ecosystems, with increases in soil N_2O emissions by predominantly denitrification process at high WFPS (Corre et al., 2014; Koehler et al., 2009; Matson et al., 2017; Werner et al., 2006). The larger stem N_2O emissions from the forest and soil N_2O emissions from both land uses in the wet than the dry seasons (Tables S2, S3) signified the favourable soil N_2O production during the wet season, which suggests that denitrification was the dominant N_2O-producing process. However, the moderate WFPS across the year (Table 4) suggests that nitrification may also have contributed to N_2O emissions, especially at Biba Yezoum (with lower rainfall and clay contents; Tables 1, S1) where the low WFPS (Table 4) likely favoured nitrification (Corre et al., 2014). For the forest, the negative correlation of the stem and soil N_2O emissions with soil NH_4^+ (Tables 3, S2) may be indicative of a conservative soil N cycle in our forest sites, as supported by the dominance of soil NH_4^+ over NO_3^- (Table 2) and by the lower soil N_2O emissions at our sites compared to NO_3^--dominated systems (Davidson et al., 2000). Although the soil mineral N content alone does not indicate the N-supplying capacity of the soil, the relative contents of NH_4^+ over NO_3^- can be a good indicator of whether the soil N cycling is conservative with low N_2O losses or increasingly leaky (Corre et al., 2010, 2014).

4.4 Land-use change effects on soil N_2O emissions

The annual soil N_2O emissions from CAF (Table 2) were comparable with those reported for rubber agroforestry in Indonesia (0.6–1.2 kg N ha^{-1} yr^{-1}; Hassler et al., 2017) and from multistrata agroforestry systems in Peru (0.6 kg N ha^{-1} yr^{-1}; Palm et al., 2002). However, our soil N_2O emissions from CAF were higher than those from an extensively managed homegarden in

503 Tanzania (0.35 N ha^{-1} yr^{-1}; Gütlein et al., 2018). In a review, Kim et al. (2016a) reported mean
504 annual N_2O emission from agroforestry systems to be 7.7 kg N ha^{-1} yr^{-1}. Most of the data used
505 in their review were from intensively managed agroforestry systems with varied fertilizer inputs,
506 which were absent in our extensively managed CAF systems. In line with this, our measured soil
507 N_2O emissions from the CAF were also lower than the emissions reported for 10–23 year old
508 CAF in Indonesia (3.1 kg N ha^{-1} yr^{-1}; Veldkamp et al., 2008). Our measured N_2O emissions
509 provide the first estimates for traditional CAF systems in Africa, as these production systems
510 were not represented in extrapolation of GHG budgets despite their extensive coverage in Africa.
511 Soil N_2O emissions did not differ between forest and CAF systems, which supported our
512 first hypothesis. This is possibly due to the presence of leguminous trees in both systems (Table
513 A1), which can compensate for N export from harvest and other losses (Erickson et al., 2002;
514 Veldkamp et al., 2008). Although studies have hinted on increased N_2O emissions from managed
515 systems that utilize leguminous trees as cover crops (Veldkamp et al., 2008), the similar
516 abundance of leguminous trees between forest and CAF at our sites may have offset this effect
517 (Table A1). Previous studies have indeed reported similar soil N_2O fluxes between reference
518 forests and unfertilized agroforestry systems (Van Lent et al., 2015). Despite the general absence
519 of heavy soil physical disturbance, cultivation and fertilization in these traditional CAF systems,
520 some soil biochemical characteristics have decreased (Table 1); however, these did not translate
521 into detectable differences in soil N_2O emissions with those from forest.

522 **4.5 Implications**

523 The biophysical conditions of our forest sites were representative of approximately two-thirds of
524 the rainforest area in the Congo Basin (1.137×10^6 km^2; Fig. B3), considering the same Ferralsol
525 soils, similar elevation (≤ 1000 m asl), and annual rainfall between 1,500 and 2,100 mm yr^{-1}.
526 Using the total (soil + stem) N_2O emission from our forest sites (1.55 ± 0.20 N_2O-N kg ha^{-1} yr^{-1};
527 Table 2), our extrapolated emission for the two-thirds of the Congo Basin was 0.18 ± 0.05 Tg

528 N_2O-N yr^{-1} (error estimate is the 95% confidence interval). This accounted 52% of the earlier
529 estimate of soil N_2O emissions from tropical rainforests in Africa (0.34 Tg N_2O-N yr^{-1}; Werner
530 et al., 2007a), or 25% based on the more recent estimate (0.72 Tg N_2O-N yr^{-1}; Valentini et al.,
531 2014). We acknowledge, however, that there are uncertainties in our extrapolation (as is the case
532 of these cited estimates) because our up-scaling approach from plot to regional level did not
533 account for the spatial variability of large-scale drivers of soil N_2O emissions, such as soil texture,
534 landforms and vegetation characteristics. These limitations of our estimate of N_2O source strength
535 for the Congo Basin rainforests call for further investigations in Africa to address the geographic
536 bias of studies in the tropical region (e.g., Powers et al., 2011). The most important consideration
537 in bottom-up spatial extrapolation approach is to recognize at the outset that the design of the
538 field quantification must reflect the landscape-scale drivers of the studied process, e.g. land-use
539 types (reflecting management), soil texture (as a surrogate of parent material) and climate are
540 landscape-scale controllers of soil N, C and GHG fluxes (e.g., Corre et al., 1999; Hassler et al.,
541 2017; Silver et al., 2000; Veldkamp et al., 2008, 2013), whereas topography (reflecting soil types,
542 moisture regimes, fertility) is the main driver within a landscape (e.g., Corre et al., 1996, 2002;
543 Groffman and Tiedje, 1989; Pennock and Corre, 2001). Process-based models and geographic
544 information system database can be combined with field-based measurements for improved
545 extrapolation.

546 Our year-round measurements of stem and soil N_2O fluxes were the first detailed study
547 carried out in the Congo Basin, with key implications on improved estimates of N_2O budget for
548 Africa. Our results revealed that trees on well-drained, highly weathered soils served as an
549 important N_2O emission pathway, with the potential to overlook up to 38% of N_2O emissions if
550 trees are not considered in the ecosystem N_2O budget. Our measured tree species spanned
551 different life history strategies and functional traits (a mixture of pioneers, non-pioneer light
552 demanders, and shade tolerants; Table A2); the lack of species-specific differences suggest that

our findings could be more widely generalisable across communities with different species compositions, at least from highly weathered soils. However, the narrow range of tree DBH classes of our measured trees may have important implications for stands of different successional stages or ages, as stem diameter size, wood density and other physiological characteristics may possibly influence stem N_2O fluxes (Machacova et al., 2019; Welch et al., 2019). Also, the possibility for large N_2O fluxes at the stem base near the ground (Barba et al., 2019; Welch et al., 2019), which we could not measure due to irregular surface of buttresses, warrants further investigation. All these combined may imply that our quantified stem N_2O emissions result in a conservative estimate of the overall stem N_2O budget from this important region. Forest conversion to traditional, mature (>20 years old) CAF systems had no effect on stem and soil N_2O emissions, because of similarities in soil moisture and soil texture, absence of fertilizer application, and comparable abundance of leguminous trees in both land uses, which can compensate for N export from harvest or other losses. Further multi-temporal and spatially replicated studies are needed to provide additional insights on the effect of forest conversion to other land uses on GHG fluxes from the African continent in order to improve GHG budget estimations for the region.

Data availability. Data available from the Göttingen Research Online repository: Iddris, N. A., Corre, M. D., Yemefack, M., van Straaten, O. and Veldkamp, E.: Stem and soil nitrous oxide fluxes from rainforest and cacao agroforest on highly weathered soils in the Congo Basin, , https://doi.org/10.25625/T2CGYM, 2020.

Author Contributions. EV and MDC conceived the research project; NAI carried out fieldwork and analyzed data; NAI and OvS performed GIS analysis; NAI and MDC interpreted data and wrote the manuscript; EV, OvS and MY revised the draft manuscript.

Competing interests. The authors declare that they have no conflict of interest.

Acknowledgements. This study was funded by the German Research Foundation (DFG, VE 219/14-1, STR 1375/1-1). We gratefully acknowledge our counterparts in Cameroon, the International Institute for Tropical Agriculture (IITA) for granting us access and use of their storage facilities. We are especially grateful to our Cameroonian field assistants Leonel Boris Gadjui Youatou, Narcis Lekeng, Yannick Eyenga Alfred, Denis Djiyo and all the field workers for their great support with field measurements, as well as Raphael Manu for helping with the GIS work and Rodine Tchiofo Lontsi for many discussions on soil processes and Cameroonian settings. We also thank the village leaders and local plot owners for granting us access to their forest and cacao farms. We thank Andrea Bauer, Kerstin Langs, Martina Knaust and Lars Szwec for their assistance with laboratory analyses.

References

Allen, R. G., Pereira, L. S., Raes, D. and Smith, M.: Determination of ET_0, crop evapotranspiration, Guidel. Comput. Crop Water Requir. Irrig. Drain. Pap. 56, 309 [online] Available from: http://www.hidmet.gov.rs/podaci/agro/table of contens_files.pdf, 1998.

Barba, J., Poyatos, R. and Vargas, R.: Automated measurements of greenhouse gases fluxes from tree stems and soils: magnitudes, patterns and drivers, Sci. Rep., 9(1), 1–13, doi:10.1038/s41598-019-39663-8, 2019.

Bouwman, A. F., Van Der Hoek, K. W. and Olivier, J. G. J.: Uncertainties in the global source distribution of nitrous oxide, J. Geophys. Res., 100(D2), 2785–2800, doi:10.1029/94JD02946, 1995.

Breuer, L., Papen, H. and Butterbach-Bahl, K.: N_2O emission from tropical forest soils of Australia, J. Geophys. Res. Atmos., 105(D21), 26353–26367, doi:10.1029/2000JD900424, 2000.

Brown, S.: Estimating biomass and biomass change of tropical forests: a primer, UN FAO Forestry Paper 134, FAO, Rome, 1997.

Castaldi, S., Bertolini, T., Valente, A., Chiti, T. and Valentini, R.: Nitrous oxide emissions from soil of an African rain forest in Ghana, Biogeosciences, 10(6), 4179–4187, doi:10.5194/bg-10-4179-2013, 2013.

Climate-Data.org: Cameroon climate, [online] Available from: https://en.climate-data.org/africa/cameroon-142/ (Accessed 21 May 2019), 2019.

Corre, M. D., van Kessel, C. and Pennock, D. J.: Landscape and Seasonal Patterns of Nitrous Oxide Emissions in a Semiarid Region, Soil Sci. Soc. Am. J., 60(6), 1806–1815, doi:10.2136/sssaj1996.03615995006000060028x, 1996.

Corre, M. D., Pennock, D. J., Van Kessel, C. and Elliott, D. K.: Estimation of annual nitrous oxide emissions from a transitional grassland-forest region in Saskatchewan, Canada, Biogeochemistry, 44(1), 29–49, doi:10.1023/A:1006025907180, 1999.

Corre, M. D., Schnabel, R. R. and Stout, W. L.: Spatial and seasonal variation of gross nitrogen transformations and microbial biomass in a Northeastern US grassland, Soil Biol. Biochem., 34(3), 445–457, doi:10.1016/S0038-0717(01)00198-5, 2002.

Corre, M. D., Dechert, G. and Veldkamp, E.: Soil nitrogen cycling following montane forest conversion in Central Sulawesi, Indonesia, Soil Sci. Soc. Am. J., 70(2), 359–366, doi:10.2136/sssaj2005.0061, 2006.

Corre, M. D., Veldkamp, E., Arnold, J. and Joseph Wright, S.: Impact of elevated N input on soil N cycling and losses in old-growth lowland and montane forests in Panama, Ecology, 91(6), 1715–1729, doi:10.1890/09-0274.1, 2010.

Corre, M. D., Sueta, J. P. and Veldkamp, E.: Nitrogen-oxide emissions from tropical forest soils exposed to elevated nitrogen input strongly interact with rainfall quantity and seasonality, Biogeochemistry, 118(1–3), 103–120, doi:10.1007/s10533-013-9908-3, 2014.

Crawley, M. J.: The R Book, John Wiley & Sons Ltd, Chichester, UK., 2009.

Curtis, J. T. and McIntosh, R. P.: An Upland Forest Continuum in the Prairie-Forest Border

627 Region of Wisconsin, Ecology, 32(3), 476–496, doi:10.2307/1931725, 1951.
628 Davidson, E. A. and Kanter, D.: Inventories and scenarios of nitrous oxide emissions, Environ.
629 Res. Lett., 9(10), doi:10.1088/1748-9326/9/10/105012, 2014.
630 Davidson, E. A. and Verchot, L. V.: Testing the hole-in-the-pipe model of nitric and nitrous
631 oxide emissions from soils using the TRAGNET database, Global Biogeochem. Cycles, 14(4),
632 1035–1043, doi:10.1029/1999GB001223, 2000.
633 Davidson, E. A., Keller, M., Erickson, H. E., Verchot, L. V. and Veldkamp, E.: Testing a
634 Conceptual Model of Soil Emissions of Nitrous and Nitric Oxides, Bioscience, 50(8), 667,
635 doi:10.1641/0006-3568(2000)050[0667:tacmos]2.0.co;2, 2000.
636 Denman, K. L., Brasseur, G., Chidthaisong, A., Ciais, P., Cox, P. M., Dickinson, R. E.,
637 Hauglustaine, D., Heinze, C., Holland, E., Jacob, D., Lohmann, U., Ramachandran, S., da
638 Silva Dias, P. L., Wofsy, S. C. and Zhang, X.: Couplings Between Changes in the Climate
639 System and Biogeochemistry, in Climate Change 2007: The Physical Science Basis.
640 Contribution of Working Group I to the Fourth Assessment Report of the Intergovernmental
641 Panel on Climate Change, Cambridge University Press, Cambridge, United Kingdom and
642 New York, NY, USA. [online] Available from:
643 https://www.ipcc.ch/site/assets/uploads/2018/02/ar4-wg1-chapter7-1.pdf, 2007.
644 Díaz-Pinés, E., Heras, P., Gasche, R., Rubio, A., Rennenberg, H., Butterbach-Bahl, K. and
645 Kiese, R.: Nitrous oxide emissions from stems of ash (Fraxinus angustifolia Vahl) and
646 European beech (Fagus sylvatica L.), Plant Soil, 398(1–2), 35–45,
647 doi:https://doi.org/10.1007/s11104-015-2629-8, 2016.
648 Dkamela, G. P.: The context of REDD+ in Cameroon: Drivers, agents and institutions,
649 Occasional., CIFOR, Bogor, Indonesia., 2010.
650 Erickson, H. E., Davidson, E. A. and Keller, M.: Former land-use and tree species affect
651 nitrogen oxide emissions from a tropical dry forest, Oecologia, 130(2), 297–308,

652 doi:10.1007/s004420100801, 2002.
653 FAO/IIASA/ISRIC/ISS-CAS/JRC: Harmonized World Soil Database (version 1.2). FAO,
654 Rome, Italy and IIASA, Laxenburg, Austria., [online] Available from:
655 http://webarchive.iiasa.ac.at/Research/LUC/External-World-soil-database/HTML/ (Accessed
656 13 September 2019), 2012.
657 Groffman, P. M. and Tiedje, J. M.: Denitrification in north temperate forest soils: Spatial and
658 temporal patterns at the landscape and seasonal scales, Soil Biol. Biochem., 21(5),
659 doi:10.1016/0038-0717(89)90053-9, 1989.
660 Groffman, P. M., Brumme, R., Butterbach-Bahl, K., Dobbie, K. E., Mosier, A. R., Ojima, D.,
661 Papen, H., Parton, W. J., Smith, K. A. and Wagner-Riddle, C.: Evaluating annual nitrous
662 oxide fluxes at the ecosystem scale, Global Biogeochem. Cycles, 14(4), 1061–1070,
663 doi:10.1029/1999GB001227, 2000.
664 Gütlein, A., Gerschlauer, F., Kikoti, I. and Kiese, R.: Impacts of climate and land use on N_2O
665 and CH_4 fluxes from tropical ecosystems in the Mt. Kilimanjaro region, Tanzania, Glob.
666 Chang. Biol., 24, 1239–1255, doi:10.1111/gcb.13944, 2018.
667 Gwanfogbe, M., Meligui, A., Moukam, J. and Nguoghia, J.: Geography of Cameroon.,
668 Macmillan Education Ltd, Hong Kong., 1983.
669 Hassler, E., Corre, M. D., Tjoa, A., Damris, M., Utami, S. R. and Veldkamp, E.: Soil fertility
670 controls soil-atmosphere carbon dioxide and methane fluxes in a tropical landscape converted
671 from lowland forest to rubber and oil palm plantations, Biogeosciences Discuss., 12(12),
672 9163–9207, doi:10.5194/bgd-12-9163-2015, 2015.
673 Hassler, E., Corre, M. D., Kurniawan, S. and Veldkamp, E.: Soil nitrogen oxide fluxes from
674 lowland forests converted to smallholder rubber and oil palm plantations in Sumatra,
675 Indonesia, Biogeosciences, 14(11), 2781–2798, doi:https://doi.org/10.5194/bg-14-2781-2017,
676 2017.

Hawthorne, W. D.: Ecological profiles of Ghanaian forest trees, Tropical forestry papers 29, 1995.

Hijmans, R. J., Cameron, S. E., Parra, J. L., Jones, P. G. and Jarvis, A.: Very high resolution interpolated climate surfaces for global land areas, Int. J. Climatol., 25(15), 1965–1978, doi:10.1002/joc.1276, 2005.

Huang, J., Golombeck, A., Prinn, R. G., Weiss, R. F., Fraser, P. J., Simmonds, P., Dlugokencky, E. J., Hall, B., Elkins, J., Steele, L. P., Langenfelds, R. L., Krummel, P. B., Dutton, G. and Porter, L.: Estimation of regional emissions of nitrous oxide from 1997 to 2005 using multinetwork measurements, a chemical transport model, and an inverse method, J. Geophys. Res. Atmos., 113(17), 1–19, doi:10.1029/2007JD009381, 2008.

IUSS Working Group WRB: World Reference Base for Soil Resources 2014, update 2015 International soil classification system for naming soils and creating legends for soil maps. World Soil Resources Reports No. 106., FAO, Rome., 2015.

Jarvis, A., Reuter, H. I., Nelson, A. and Guevara, E.: Hole-filled SRTM for the globe, Version 4. CGIAR-CSI SRTM 90m Database, Int. Cent. Trop. Agric. Cali, Columbia. http//srtm.csi.cgiar.org, (September 2017), 2008.

Kiese, R., Hewett, B., Graham, A. and Butterbach-Bahl, K.: Seasonal variability of N_2O emissions and CH_4 uptake by tropical rainforest soils of Queensland, Australia, Global Biogeochem. Cycles, 17(2), 1043, doi:10.1029/2002gb002014, 2003.

Kim, D. G., Kirschbaum, M. U. F. and Beedy, T. L.: Carbon sequestration and net emissions of CH_4 and N_2O under agroforestry: Synthesizing available data and suggestions for future studies, Agric. Ecosyst. Environ., 226, 65–78, doi:10.1016/j.agee.2016.04.011, 2016a.

Kim, D. G., Thomas, A. D., Pelster, D. E., Rosenstock, T. S. and Sanz-Cobena, A.: Greenhouse gas emissions from natural ecosystems and agricultural lands in sub-Saharan Africa: Synthesis of available data and suggestions for further research, Biogeosciences, 13(16), 4789–4809,

doi:10.5194/bg-13-4789-2016, 2016b.

Koehler, B., Corre, M. D., Veldkamp, E., Wullaert, H. and Wright, S. J.: Immediate and long-term nitrogen oxide emissions from tropical forest soils exposed to elevated nitrogen input, Glob. Chang. Biol., 15(8), 2049–2066, doi:10.1111/j.1365-2486.2008.01826.x, 2009.

Kotto, J. S., Moukam, A., Njomgang, R., Tiki-Manga, T., Tonye, J., Diaw, C., Gockowski, J., Hauser, S., Weise, S. F., Nwaga, D., Zapfack, L., Palm, C. A., Woomer, P., Gillison, A., Bignell, D. and Tondoh, J.: Alternatives to slash-and-burn in Indonesia: summary report & synthesis of phase II in Cameroon, Nairobi. Kenya., 2002.

Kreuzwieser, J., Buchholz, J. and Rennenberg, H.: Emission of Methane and Nitrous Oxide by Australian Mangrove Ecosystems, Plant Biol., 5(4), 423–431, doi:10.1055/s-2003-42712, 2003.

Kroetsch, D. and Wang, C.: Particle size distribution, in Soil Sampling and Methods of Analysis, Second Edition, pp. 713–725., 2008.

Lenhart, K., Behrendt, T., Greiner, S., Steinkamp, J., Well, R., Giesemann, A. and Keppler, F.: Nitrous oxide effluxes from plants as a potentially important source to the atmosphere, New Phytol., 221(3), 1398–1408, doi:10.1111/nph.15455, 2019.

Van Lent, J., Hergoualc'H, K. and Verchot, L. V.: Reviews and syntheses: Soil N_2O and NO emissions from land use and land-use change in the tropics and subtropics: A meta-analysis, Biogeosciences, 12(23), 7299–7313, doi:10.5194/bg-12-7299-2015, 2015.

Machacova, K., Papen, H., Kreuzwieser, J. and Rennenberg, H.: Inundation strongly stimulates nitrous oxide emissions from stems of the upland tree Fagus sylvatica and the riparian tree Alnus glutinosa, Plant Soil, 364(1–2), 287–301, doi:10.1007/s11104-012-1359-4, 2013.

Machacova, K., Bäck, J., Vanhatalo, A., Halmeenmäki, E., Kolari, P., Mammarella, I., Pumpanen, J., Acosta, M., Urban, O. and Pihlatie, M.: Pinus sylvestris as a missing source of nitrous oxide and methane in boreal forest, Sci. Rep., 6(March), 1–8, doi:10.1038/srep23410,

2016.

Machacova, K., Maier, M., Svobodova, K., Lang, F. and Urban, O.: Cryptogamic stem covers may contribute to nitrous oxide consumption by mature beech trees, Sci. Rep., 7(1), 1–7, doi:10.1038/s41598-017-13781-7, 2017.

Machacova, K., Vainio, E., Urban, O. and Pihlatie, M.: Seasonal dynamics of stem N_2O exchange follow the physiological activity of boreal trees, Nat. Commun., 10(1), 1–13, doi:10.1038/s41467-019-12976-y, 2019.

Matson, A. L., Corre, M. D., Langs, K. and Veldkamp, E.: Soil trace gas fluxes along orthogonal precipitation and soil fertility gradients in tropical lowland forests of Panama, Biogeosciences, 14(14), 3509–3524, doi:10.5194/bg-14-3509-2017, 2017.

McJannet, D., Fitch, P., Disher, M. and Wallace, J.: Measurements of transpiration in four tropical rainforest types of north Queensland, Australia, Hydrol. Process., 21, 3549–3564, doi:https://doi.org/10.1002/hyp.6576, 2007.

Müller, A. K., Matson, A. L., Corre, M. D. and Veldkamp, E.: Soil N_2O fluxes along an elevation gradient of tropical montane forests under experimental nitrogen and phosphorus addition, Front. Earth Sci., 3(October), 1–12, doi:10.3389/feart.2015.00066, 2015.

Neill, C., Steudler, P. A., Garcia-Montiel, D. C., Melillo, J. M., Feigl, B. J., Piccolo, M. C. and Cerri, C. C.: Rates and controls of nitrous oxide and nitric oxide emissions following conversion of forest to pasture in Rondônia, Nutr. Cycl. Agroecosystems, 71(1), 1–15, doi:10.1007/s10705-004-0378-9, 2005.

O'Brien, J. J., Oberbauer, S. F. and Clark, D. B.: Whole tree xylem sap flow responses to multiple environmental variables in a wet tropical forest, Plant, Cell Environ., 27(5), 551–567, doi:10.1111/j.1365-3040.2003.01160.x, 2004.

Palm, C. A., Alegre, J. C., Arevalo, L., Mutuo, P. K., Mosier, A. R. and Coe, R.: Nitrous oxide and methane fluxes in six different land use systems in the Peruvian Amazon, Global

752 Biogeochem. Cycles, 16(4), 1073, doi:10.1029/2001gb001855, 2002.
753 Pennock, D. J. and Corre, M. D.: Development and application of landform segmentation
754 procedures, Soil Tillage Res., 58(3–4), 151–162, doi:10.1016/S0167-1987(00)00165-3, 2001.
755 Powers, J. S., Corre, M. D., Twine, T. E. and Veldkamp, E.: Geographic bias of field
756 observations of soil carbon stocks with tropical land-use changes precludes spatial
757 extrapolation, Proc. Natl. Acad. Sci. U. S. A., 108(15), 6318–6322,
758 doi:10.1073/pnas.1016774108, 2011.
759 Purbopuspito, J., Veldkamp, E., Brumme, R. and Murdiyarso, D.: Trace gas fluxes and nitrogen
760 cycling along an elevation sequence of tropical montane forests in Central Sulawesi,
761 Indonesia, Global Biogeochem. Cycles, 20(3), 1–11, doi:10.1029/2005GB002516, 2006.
762 Ravishankara, A. R., Daniel, J. S. and Portmann, R. W.: Nitrous oxide (N_2O): The dominant
763 ozone-depleting substance emitted in the 21st century, Science (80-.)., 326(5949), 123–125,
764 doi:10.1126/science.1176985, 2009.
765 Rusch, H. and Rennenberg, H.: Black alder (Alnus glutinosa (L.) Gaertn.) trees mediate
766 methane and nitrous oxide emission from the soil to the atmosphere, Plant Soil, 201(1), 1–7,
767 doi:10.1023/A:1004331521059, 1998.
768 Saj, S., Jagoret, P. and Todem Ngogue, H.: Carbon storage and density dynamics of associated
769 trees in three contrasting Theobroma cacao agroforests of Central Cameroon, Agrofor. Syst.,
770 87(6), 1309–1320, doi:10.1007/s10457-013-9639-4, 2013.
771 Serca, D., Delmas, R., Jambert, C. and Labroue, L.: Emissions of nitrogen oxides from
772 equatorial rain forest in central Africa:, Tellus B Chem. Phys. Meteorol., 46(4), 243–254,
773 doi:10.3402/tellusb.v46i4.15795, 1994.
774 Silver, W. L., Neff, J., McGroddy, M., Veldkamp, E., Keller, M. and Cosme, R.: Effects of Soil
775 Texture on Belowground Carbon and Nutrient Storage in a Lowland Amazonian Forest
776 Ecosystem, Ecosystems, 3(2), 193–209, doi:10.1007/s100210000019, 2000.

Sonwa, D. J., Nkongmeneck, B. A., Weise, S. F., Tchatat, M., Adesina, A. A. and Janssens, M. J. J.: Diversity of plants in cocoa agroforests in the humid forest zone of Southern Cameroon, Biodivers. Conserv., 16(8), 2385–2400, doi:10.1007/s10531-007-9187-1, 2007.

van Straaten, O., Corre, M. D., Wolf, K., Tchienkoua, M., Cuellar, E., Matthews, R. B. and Veldkamp, E.: Conversion of lowland tropical forests to tree cash crop plantations loses up to one-half of stored soil organic carbon, Proc. Natl. Acad. Sci., 112(32), 9956–9960, doi:10.1073/pnas.1504628112, 2015.

Tchiofo Lontsi, R., Corre, M. D., van Straaten, O. and Veldkamp, E.: Changes in soil organic carbon and nutrient stocks in conventional selective logging versus reduced-impact logging in rainforests on highly weathered soils in Southern Cameroon, For. Ecol. Manage., 451(August), 117522, doi:10.1016/j.foreco.2019.117522, 2019.

Thompson, R. L., Chevallier, F., Crotwell, A. M., Dutton, G., Langenfelds, R. L., Prinn, R. G., Weiss, R. F., Tohjima, Y., Nakazawa, T., Krummel, P. B., Steele, L. P., Fraser, P. J., O'doherty, S., Ishijima, K. and Aoki, S.: Nitrous oxide emissions 1999 to 2009 from a global atmospheric inversion, Atmos. Chem. Phys., 14(4), 1801–1817, doi:10.5194/acp-14-1801-2014, 2014.

Valentini, R., Arneth, A., Bombelli, A., Castaldi, S., Cazzolla Gatti, R., Chevallier, F., Ciais, P., Grieco, E., Hartmann, J., Henry, M., Houghton, R. A., Jung, M., Kutsch, W. L., Malhi, Y., Mayorga, E., Merbold, L., Murray-Tortarolo, G., Papale, D., Peylin, P., Poulter, B., Raymond, P. A., Santini, M., Sitch, S., Vaglio Laurin, G., Van Der Werf, G. R., Williams, C. A. and Scholes, R. J.: A full greenhouse gases budget of africa: Synthesis, uncertainties, and vulnerabilities, Biogeosciences, 11(2), 381–407, doi:10.5194/bg-11-381-2014, 2014.

Veldkamp, E.: Organic Carbon Turnover in Three Tropical Soils under Pasture after Deforestation, Soil Sci. Soc. Am. J., 58(1), 175–180, doi:10.2136/sssaj1994.03615995005800010025x, 1994.

802 Veldkamp, E., Purbopuspito, J., Corre, M. D., Brumme, R. and Murdiyarso, D.: Land use
803 change effects on trace gas fluxes in the forest margins of Central Sulawesi, Indonesia, J.
804 Geophys. Res. Biogeosciences, 113(2), 1–11, doi:10.1029/2007JG000522, 2008.
805 Veldkamp, E., Koehler, B. and Corre, M. D.: Indications of nitrogen-limited methane uptake in
806 tropical forest soils, Biogeosciences, 10(8), 5367–5379, doi:10.5194/bg-10-5367-2013, 2013.
807 Veldkamp, E., Schmidt, M., Powers, J. S. and Corre, M. D.: Deforestation and reforestation
808 impacts on soils in the tropics, Nat. Rev. Earth Environ., 1–16, 2020.
809 Verchot, L. V., Hutabarat, L., Hairiah, K. and van Noordwijk, M.: Nitrogen availability and soil
810 N_2O emissions following conversion of forests to coffee in southern Sumatra, Global
811 Biogeochem. Cycles, 20(4), 1–12, doi:10.1029/2005GB002469, 2006.
812 Wanyama, I., Pelster, D. E., Arias-Navarro, C., Butterbach-Bahl, K., Verchot, L. V. and Rufino,
813 M. C.: Management intensity controls soil N_2O fluxes in an Afromontane ecosystem, Sci.
814 Total Environ., 624(December), 769–780, doi:10.1016/j.scitotenv.2017.12.081, 2018.
815 Welch, B., Gauci, V. and Sayer, E. J.: Tree stem bases are sources of CH_4 and N_2O in a tropical
816 forest on upland soil during the dry to wet season transition, Glob. Chang. Biol., 25(1), 361–
817 372, doi:10.1111/gcb.14498, 2019.
818 Wen, Y., Corre, M. D., Rachow, C., Chen, L. and Veldkamp, E.: Nitrous oxide emissions from
819 stems of alder, beech and spruce in a temperate forest, Plant Soil, doi:10.1007/s11104-017-
820 3416-5, 2017.
821 Werner, C., Zheng, X., Tang, J., Xie, B., Liu, C., Kiese, R. and Butterbach-Bahl, K.: N_2O, CH_4
822 and CO_2 emissions from seasonal tropical rainforests and a rubber plantation in Southwest
823 China, Plant Soil, 289(1–2), 335–353, doi:10.1007/s11104-006-9143-y, 2006.
824 Werner, C., Butterbach-Bahl, K., Haas, E., Hickler, T. and Kiese, R.: A global inventory of
825 N_2O emissions from tropical rainforest soils using a detailed biogeochemical model, Global
826 Biogeochem. Cycles, 21(3), doi:10.1029/2006GB002909, 2007a.

827 Werner, C., Kiese, R. and Butterbach-Bahl, K.: Soil-atmosphere exchange of N_2O, CH_4, and
828 CO_2 and controlling environmental factors for tropical rain forest sites in western Kenya, J.
829 Geophys. Res., 112(3), D03308, doi:10.1029/2006JD007388, 2007b.
830 Wolf, K., Veldkamp, E., Homeier, J. and Martinson, G. O.: Nitrogen availability links forest
831 productivity, soil nitrous oxide and nitric oxide fluxes of a tropical montane forest in southern
832 Ecuador, Global Biogeochem. Cycles, 25(4), GB4009, doi:10.1029/2010GB003876, 2011.
833 Zanne, A. E., Lopez-Gonzalez, G., Coomes, David A., Ilic, J., Jansen, S., Lewis, S. L., Miller,
834 R. B., Swenson, N. G., Wiemann, M. C. and Chave, J.: Data from: Towards a worldwide
835 wood economics spectrum, v5, Dryad, Dataset, https://doi.org/10.5061/dryad.234, 2009.
836 Zapfack, L., Engwald, S., Sonké, B., Achoundong, G. and Madong, B. A.: The impact of land
837 conversion on plant biodiversity in the forest zone of Cameroon, Biodivers. Conserv., 11(11),
838 2047–2061, doi:https://doi.org/10.1023/A:1020861925294, 2002.

Tables

839 **Table 1.** Mean (±SE, $n = 4$) soil biochemical characteristics in the top 50 cm[a] depth in forest and
840 cacao agroforestry (CAF) within each site in the Congo Basin, Cameroon. Means followed by
841 different lowercase letters indicate significant differences between land-use types within each site
842 and different capital letters indicate significant differences among the three sites within a land-
843 use type (Anova with Tukey's HSD test or Kruskal-Wallis ANOVA with multiple comparison
844 extension test at $P \leq 0.05$).

Soil characteristics	Aloum site		Biba Yezoum site		Tomba site	
	Forest	CAF	Forest	CAF	Forest	CAF
Clay (30-50 cm) (%)	$66.0 \pm 2.4^{a,A}$	$59.3 \pm 6.1^{a,A}$	$32.8 \pm 9.4^{a,B}$	$39.5 \pm 0.9^{a,B}$	$55.3 \pm 0.5^{a,AB}$	$51.8 \pm 1.1^{a,AB}$
Bulk density (g cm^{-3})	$1.2 \pm 0.1^{a,A}$	$1.2 \pm 0.1^{a,A}$	$1.2 \pm 0.1^{a,A}$	$1.2 \pm 0.1^{a,A}$	$1.2 \pm 0.1^{a,A}$	$1.2 \pm 0.1^{a,A}$
pH (1:4 H_2O)	$3.7 \pm 0.0^{b,A}$	$4.1 \pm 0.1^{a,A}$	$3.7 \pm 0.1^{b,A}$	$4.6 \pm 0.2^{a,A}$	$3.6 \pm 0.0^{b,A}$	$4.5 \pm 0.2^{a,A}$
^{15}N natural abundance (‰)	$8.4 \pm 0.2^{b,A}$	$10.2 \pm 0.1^{a,A}$	$8.6 \pm 0.2^{a,A}$	$9.1 \pm 0.2^{a,B}$	$8.8 \pm 0.1^{a,A}$	$8.8 \pm 0.1^{a,B}$
Soil organic C (kg C m^{-2})	$12.1 \pm 0.4^{a,A}$	$6.7 \pm 0.2^{b,A}$	$7.2 \pm 0.9^{a,B}$	$5.6 \pm 0.7^{a,A}$	$9.8 \pm 0.2^{a,AB}$	$7.1 \pm 0.4^{b,A}$
Total N (kg N m^{-2})	$1.1 \pm 0.1^{a,A}$	$0.7 \pm 0.0^{b,A}$	$0.7 \pm 0.1^{a,A}$	$0.5 \pm 0.0^{a,B}$	$0.9 \pm 0.0^{a,A}$	$0.7 \pm 0.0^{b,A}$
ECEC[b] ($mmol_c$ kg^{-1})	$57.5 \pm 3.9^{a,A}$	$33.9 \pm 2.8^{b,A}$	$49.1 \pm 11.3^{a,A}$	$41.1 \pm 7.2^{a,A}$	$58.5 \pm 2.0^{a,A}$	$46.8 \pm 4.7^{a,A}$
Exch. bases[b] ($mmol_c$ kg^{-1})	$3.5 \pm 0.3^{b,B}$	$8.7 \pm 1.7^{a,B}$	$8.5 \pm 1.1^{b,A}$	$31.0 \pm 8.5^{a,A}$	$9.3 \pm 0.8^{b,A}$	$30.4 \pm 7.6^{a,A}$
Exchangeable Al ($mmol_c$ kg^{-1})	$47.3 \pm 3.1^{a,A}$	$20.9 \pm 3.5^{b,A}$	$32.9 \pm 8.9^{a,A}$	$5.4 \pm 1.2^{b,B}$	$39.2 \pm 2.3^{a,A}$	$12.3 \pm 2.7^{b,AB}$

845 [a] Values are depth-weighted average, except for clay content (30–50 cm) and stocks of soil
846 organic C and total N, which are sum of the entire 50-cm depth. [b] ECEC: effective cation
847 exchange capacity; Exch. bases: sum of exchangeable Ca, Mg, K, Na.

Table 2. Mean (±SE, $n = 4$) stem and soil N_2O emission as well as annual stem, soil, and total (soil + stem) N_2O fluxes from forest and cacao agroforestry (CAF) within each site in the Congo Basin, Cameroon. Means followed by different lowercase letters indicate significant differences between land-use types within each site and different capital letters indicate significant differences among the three sites within a land-use type (linear mixed-effect models with Tukey's HSD at $P \leq 0.05$).

Site/ Land-use type	Stem N_2O fluxes (µg N m^{-2} stem h^{-1})	Annual stem N_2O fluxes[a] (kg N ha^{-1} yr^{-1})	Soil N_2O fluxes (µg N m^{-2} soil h^{-1})	Annual soil N_2O fluxes[a] (kg N ha^{-1} yr^{-1})	Total (soil + stem) N_2O flux (kg N ha^{-1} yr^{-1})	Contribution of stem to total N_2O flux (%)
Aloum						
Forest	1.13 ± 0.22[a,A]	0.13 ± 0.00	13.7 ± 2.2[a,A]	0.87 ± 0.14	1.00 ± 0.14	13.7 ± 1.8
CAF	0.90 ± 0.16[a,A]	0.09 ± 0.01 (0.02 ± 0.01)	15.2 ± 2.8[a,A]	1.06 ± 0.17	1.15 ± 0.17	7.8 ± 1.6
Biba Yezoum						
Forest	2.38 ± 0.48[a,A]	0.87 ± 0.05	17.2 ± 2.9[a,A]	1.46 ± 0.23	2.33 ± 0.24	38.2 ± 3.5
CAF	1.11 ± 0.21[a,A]	0.12 ± 0.01 (0.03 ± 0.01)	10.6 ± 2.1[a,A]	0.80 ± 0.20	0.92 ± 0.20	14.8 ± 3.0
Tomba						
Forest	0.89 ± 0.10[a,A]	0.14 ± 0.01	15.0 ± 1.7[a,A]	1.18 ± 0.18	1.31 ± 0.18	11.4 ± 2.2
CAF	0.90 ± 0.12[a,A]	0.12 ± 0.00 (0.05 ± 0.02)	15.8 ± 2.0[a,A]	1.25 ± 0.14	1.37 ± 0.14	8.9 ± 0.9

[a] Annual stem and soil N_2O fluxes were not statistically tested for differences among sites or between land-use types since these annual values are trapezoidal extrapolations. Annual stem N_2O emissions in parentheses are from cacao trees only.

857 **Table 3.** Spearman correlation coefficients of stem N_2O flux (μg N m^{-2} stem h^{-1}) and soil N_2O
858 flux (μg N m^{-2} soil h^{-1}) with air temperature (°C), water-filled pore space (WFPS) (%, top 5
859 cm depth), extractable NH_4^+ (mg N kg^{-1}, top 5 cm depth), soil-air N_2O concentration (ppm N_2O
860 at 50 cm depth), and vapour pressure deficit (VPD) (kPa), using the monthly means of the four
861 replicate plots per land use across the three sites from May 2017 to April 2018 (n = 33).

Land use	Variable	Soil N_2O flux	Air temp.	WFPS	NH_4^+	Soil-air N_2O concentration	VPD
Forest	Stem N_2O flux	0.25	0.39[b]	−0.41[b]	−0.57[a]	0.41[b]	0.62[a]
	Soil N_2O flux		−0.07	0.15	−0.43[b]	0.55[a]	−0.01
CAF	Stem N_2O flux	0.60[a]	−0.29	0.17	−0.26	0.21	0.21
	Soil N_2O flux		−0.34[b]	0.53[a]	−0.14	0.51[a]	0.10

[b] $P \leq 0.05$, [a] $P \leq 0.01$.

862 **Table 4.** Mean (±SE, n = 4) water-filled pore space (WFPS) and extractable mineral N in the
863 top 5 cm of soil in forest and cacao agroforestry (CAF) within each site in Congo Basin,
864 Cameroon, measured monthly from May 2017 to April 2018.

Site/ Land-use type[a]	WFPS (%)	NH_4^+ (mg N kg^{-1})	NO_3^- (mg N kg^{-1})
Aloum			
Forest	$64.3 \pm 3.6^{a,A}$	$7.3 \pm 1.0^{a,A}$	$6.3 \pm 1.2^{a,A}$
CAF	$56.4 \pm 2.5^{a,A}$	$5.1 \pm 0.8^{a,B}$	$2.4 \pm 0.6^{b,A}$
Biba Yezoum			
Forest	$41.5 \pm 2.7^{a,B}$	$4.9 \pm 0.4^{b,B}$	$2.9 \pm 0.5^{a,B}$
CAF	$32.6 \pm 2.7^{a,B}$	$7.3 \pm 0.4^{a,A}$	$2.7 \pm 0.6^{a,A}$
Tomba			
Forest	$48.3 \pm 3.0^{a,B}$	$7.6 \pm 0.6^{a,A}$	$5.8 \pm 1.0^{a,A}$
CAF	$52.3 \pm 5.1^{a,A}$	$7.1 \pm 0.6^{a,A}$	$2.8 \pm 0.6^{b,A}$

865 [a] Means followed by different lowercase letters indicate significant differences between land-
866 use types within each site and different capital letters indicate significant differences among the
867 three sites within a land-use type (linear mixed-effect models with Tukey's HSD at $P \leq 0.05$).

Figures

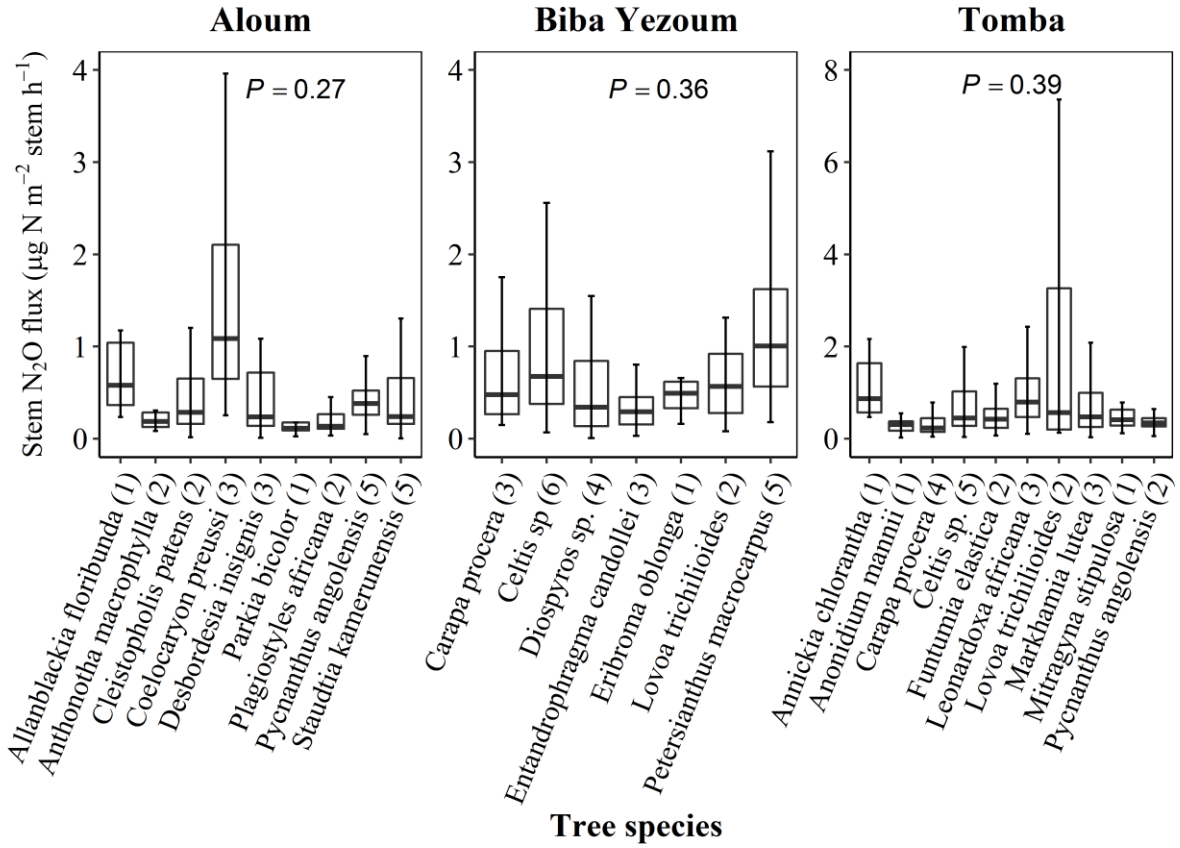

Figure 1. Stem N_2O fluxes from 22 tree species at three forest sites (Aloum, Biba Yezoum and Tomba) across central and south Cameroon in the Congo Basin. Boxes (25^{th}, median and 75^{th} percentile) and whiskers (1.5 × interquartile range) are based on N_2O fluxes measured monthly from May 2017 to April 2018 for each tree species, and the values in parentheses represent the number of trees measured per species. There were no differences in N_2O fluxes among species (linear mixed-effect models with Tukey's HSD at $P \geq 0.27$).

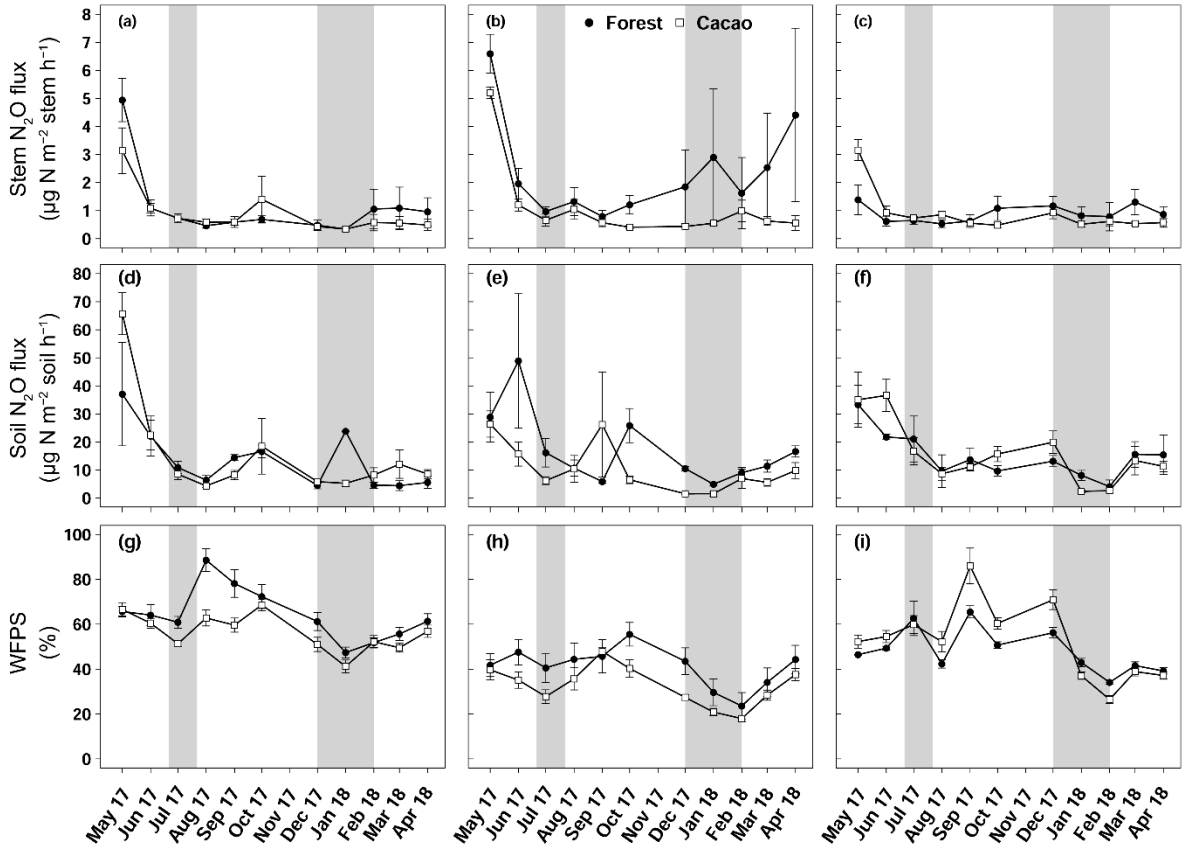

874 **Figure 2.** Mean (±SE, *n* = 4) stem N_2O fluxes (top panel), soil N_2O fluxes (middle panel) and
875 water-filled pore space (bottom panel) in Aloum site (a, d and g), Biba Yezoum site (b, e and
876 h) and Tomba site (c, f and i) in the Congo Basin, Cameroon, measured monthly from May
877 2017 to April 2018; grey shadings mark the dry season.

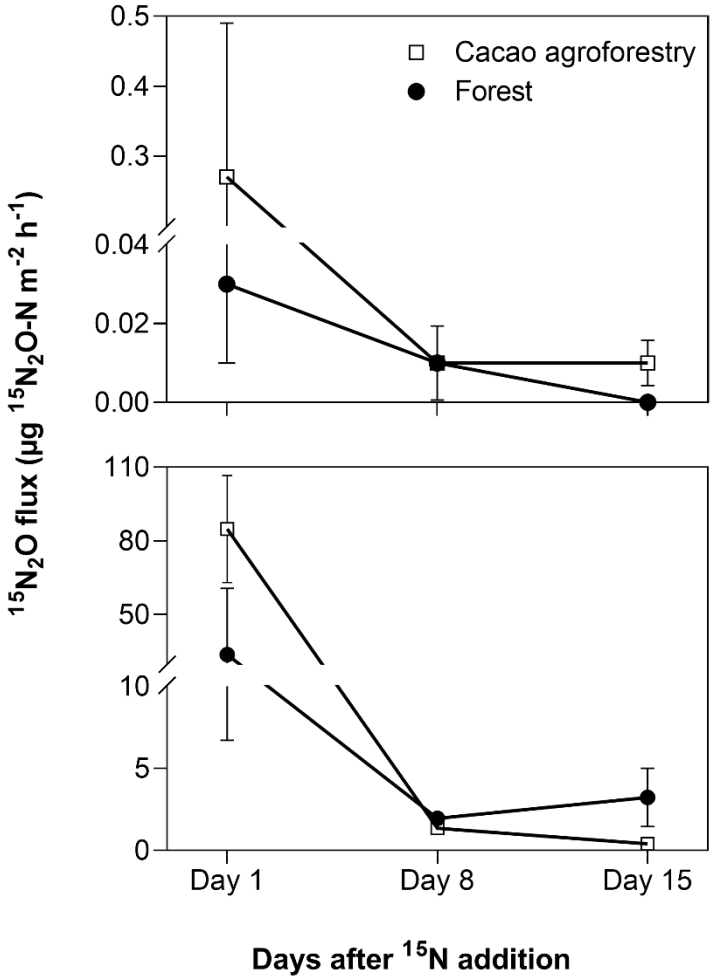

878 **Figure 3.** Mean (±SE, *n* = 3) $^{15}N_2O$ fluxes from stems (top panel, unit is per m^2 stem area) and
879 soil (bottom panel, unit is m^{-2} ground area) in the Congo Basin, Cameroon. In May 2018, 290
880 mg ^{15}N (in the form of $(^{15}NH_4)_2SO_4$ with 98% ^{15}N) was dissolved in 8 L distilled water and
881 sprayed within 0.8 m^2 area around each tree (equal to 10 mm rain), which was only 20 % of the
882 extant mineral N in the top 10 cm soil and 49 ± 1% and 52 ± 2% water-filled pore space for the
883 forest and CAF, respectively, comparable to the soil water content of the site (Fig. 2).

Appendices

884 **Table A1.** Vegetation and site characteristics of the study sites on highly weathered soils in the
885 Congo Basin, Cameroon. All vegetation characteristics were determined from trees with ≥ 10
886 cm diameter at breast height in both forest and cacao agroforestry.

Site	**Aloum**		**Biba Yezoum**		**Tomba**	
Land use	Forest	Cacao agroforestry[a]	Forest	Cacao agroforestry[a]	Forest	Cacao agroforestry[a]
Tree density (n ha^{-1})	594 ± 29	403 ± 60 (140 ± 37)	619 ± 16	267 ± 24 (96 ± 16)	453 ± 34	430 ± 51 (292 ± 79)
Total basal area (m^2 ha^{-1})	35 ± 1.4	27 ± 2.5 (1.5 ± 0.5)	33 ± 2.9	27 ± 2.0 (0.9 ± 0.2)	34 ± 2.3	30 ± 3.2 (3.8 ± 1.3)
Legume abundance (% of the number of trees)	7.7 ± 1.7	5.9 ± 1.4	9.3 ± 1.9	6.5 ± 2.3	7.4 ± 1.6	4.8 ± 1.4
Tree height (m)	18.6 ± 0.5	15.1 ± 0.9 (6.8 ± 0.1)	20.6 ± 0.5	16.1 ± 0.4 (6.2 ± 0.3)	19.5 ± 0.4	11.7 ± 1.7 (6.1 ± 0.3)
Diameter at breast height (cm)	23.2 ± 0.6	23.3 ± 1.6 (11.4 ± 0.2)	22.6 ± 0.8	27.2 ± 0.2 (10.8 ± 0.2)	24.8 ± 1.0	23.5 ± 2.7 (12.3 ± 0.6)
Elevation (m above sea level)		651		674		752
Precipitation[b] (mm yr^{-1}; from 1982 to 2012)		2064		1639		1577

887 [a] For cacao agroforestry, the first values are for both cacao and remnant shade trees, and the
888 second values in parentheses are for cacao trees only. [b] Climate-Data.org, 2019.

Table A2. Ecological and functional traits of the measured trees, selected from the most dominant tree species at each site, based on their Importance Value Index (IVI = relative density + relative frequency + relative dominance; Curtis and McIntosh, 1951). For a given species, the relative density refers to its total number of individuals in the four forest plots at each site; the relative frequency refers to its occurrence among the four forest plots; and the relative dominance refers to its total basal area in the four forest plots, all expressed as percentages of all species.

Site	Guild[a]	Phenology	Dispersal	Wood density[b]
Aloum				
Allanblackia floribunda	SB	Evergreen	Zoochore	0.69
Anthonotha macrophylla	SB	Evergreen	–	0.83
Cleistopholis patens	Pioneer	Deciduous	Zoochore	0.34
Coelocaryon preussi	NPLD	Evergreen	Zoochore	0.50
Desbordesia insignis	SB	Evergreen	Anemochore	0.92
Parkia bicolor	NPLD	Deciduous	Zoochore	0.45
Plagiostyles africana	SB	Evergreen	Zoochore	0.75
Pycnanthus angolensis	NPLD	Evergreen	Zoochore	0.41
Staudtia kamerunensis	SB	Evergreen	Zoochore	0.79
Theobroma cacao	Sub-canopy	Evergreen		0.42
Biba Yezoum				
Carapa procera	SB	Evergreen	Zoochore	0.60
Celtis sp	NPLD + SB	Deciduous + Evergreen	Zoochore	0.59
Diospyros sp	SB	Deciduous	Zoochore	0.70
Entandrophragma candollei	NPLD	Deciduous	Anemochore	0.57
Eribroma oblongum	SB	Deciduous	Zoochore	0.64
Lovoa trichilioides	NPLD	Evergreen	Anemochore	0.46
Petersianthus macrocarpus	Pioneer	Deciduous + Evergreen	Anemochore	0.68
Theobroma cacao	Sub-canopy	Evergreen		0.42
Tomba				
Annickia chlorantha	SB	Evergreen	Zoochore	0.44
Anonidium mannii	SB	Evergreen	Zoochore	0.29
Carapa procera	SB	Evergreen	Zoochore	0.60
Celtis sp.	NPLD + SB	Deciduous + Evergreen	Zoochore	0.59
Funtumia elastica	NPLD	Evergreen	Anemochore	0.42
Leonardoxa africana	SB	–	–	–
Lovoa trichilioides	NPLD	Evergreen	Anemochore	0.46
Markhamia lutea	Pioneer	Evergreen	Anemochore	0.50
Mitragyna stipulosa	Pioneer	Evergreen	Anemochore	0.47
Pycnanthus angolensis	NPLD	Evergreen	Zoochore	0.41
Theobroma cacao	Sub-canopy	Evergreen		0.42

[a] Each species was assigned to one of the three regeneration guilds defined by Hawthorne (1995): SB: shade-bearer, NPLD: non-pioneer light demander, P: pioneer. [b] Global Wood Density Database (Brown et al., 1997; Zanne et al., 2009).

899 **Table A3.** Seasonal mean (±SE, n = 4) water-filled pore space (WFPS), extractable mineral N
900 (measured in the top 5 cm of soil) and nitrous oxide (N_2O) fluxes in forests on highly weathered
901 soils in the Congo Basin, Cameroon. Means followed by different lowercase letters indicate
902 significant differences between seasons for each site (linear mixed-effect models with Tukey's
903 HSD at $P \leq 0.05$).

Season/ site	Stem N_2O flux (µg N m^{-2} stem h^{-1})	Soil N_2O flux (µg N m^{-2} soil h^{-1})	WFPS (%)	Soil NH_4^+ (mg N kg^{-1})	Soil NO_3^- (mg N kg^{-1})
Wet season					
Aloum	1.56 ± 0.36[a]	16.7 ± 3.7[a]	66.2 ± 2.2[a]	6.0 ± 0.6[a]	6.0 ± 0.8[a]
Biba Yezoum	2.92 ± 0.73[a]	22.9 ± 4.9[a]	44.8 ± 2.6[a]	4.4 ± 0.3[a]	2.2 ± 0.2[b]
Tomba	1.01 ± 0.13[a]	18.6 ± 2.2[a]	49.4 ± 1.8[a]	6.9 ± 0.5[b]	5.4 ± 0.8[a]
Dry season					
Aloum	0.61 ± 0.14[b]	10.0 ± 1.8[b]	62.0 ± 3.6[a]	8.7 ± 1.3[a]	6.6 ± 1.0[a]
Biba Yezoum	1.73 ± 0.57[b]	10.3 ± 1.4[b]	36.3 ± 3.2[a]	5.5 ± 0.4[a]	3.6 ± 0.5[a]
Tomba	0.69 ± 0.15[b]	8.9 ± 1.9[b]	46.2 ± 3.1[a]	8.7 ± 0.8[a]	6.5 ± 1.1[a]

Table A4. Seasonal mean (±SE, $n = 4$) water-filled pore space (WFPS), extractable mineral N (measured in the top 5 cm of soil) and nitrous oxide (N_2O) fluxes in cacao agroforestry sites located on highly weathered soils in the Congo Basin, Cameroon. Means followed by different lowercase letters indicate significant differences between seasons for each site (linear mixed-effect models with Tukey's HSD at $P \leq 0.05$).

Site/ season	Stem N_2O flux (μg N m^{-2} stem h^{-1})	Soil N_2O flux (μg N m^{-2} soil h^{-1})	WFPS (%)	Soil NH_4^+ (mg N kg^{-1})	Soil NO_3^- (mg N kg^{-1})
Wet season					
Aloum	1.21 ± 0.27^a	22.6 ± 4.7^a	60.3 ± 1.6^a	4.3 ± 0.4^a	2.1 ± 0.4^a
Biba Yezoum	1.43 ± 0.36^a	15.0 ± 3.5^a	38.2 ± 1.7^a	7.0 ± 0.6^a	2.2 ± 0.4^a
Tomba	1.05 ± 0.18^a	21.2 ± 2.6^a	53.4 ± 2.4^a	7.3 ± 0.8^a	2.5 ± 0.3^a
Dry season					
Aloum	0.53 ± 0.07^b	6.4 ± 0.7^b	51.7 ± 1.9^b	6.0 ± 1.0^a	2.7 ± 0.6^a
Biba Yezoum	0.74 ± 0.12^a	5.3 ± 1.3^b	25.9 ± 1.8^b	7.5 ± 0.6^a	3.2 ± 0.7^a
Tomba	0.63 ± 0.06^a	6.2 ± 1.2^b	50.4 ± 6.2^a	6.9 ± 0.9^a	3.4 ± 0.7^a

Appendix B1. Location of the study sites in Cameroon, showing the four replicate plots per land use (green for forests and orange for cacao agroforestry) at one site.

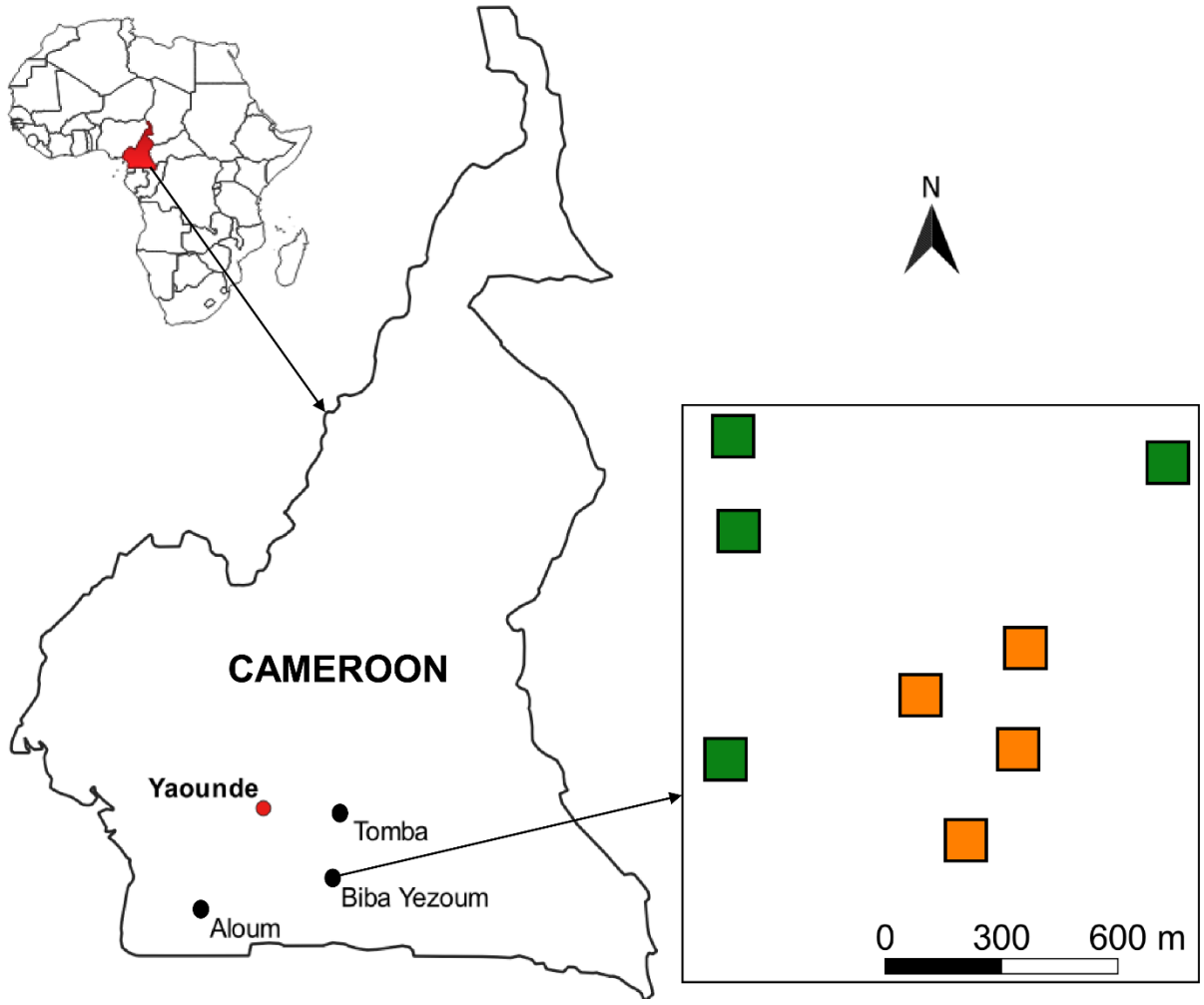

Appendix B2. Sampling set-up for stem nitrous oxide (N_2O)-flux measurement at three stem heights in a rainforest in the Congo Basin, Cameroon.

Appendix B3. Map of the Congo Basin rainforest (green) spanning across the six major Congo Basin countries. Brown shaded area represents the proportion of the Congo rainforest with similar biophysical conditions as our study sites (Ferralsol soils, ≤ 1000 m elevation, and 1500–2100 mm yr^{-1} precipitation).